

Flavour violation in a supersymmetric T' model

Luca Merlo,^{a,b} Stefano Rigolin^c and Bryan Zaldivar^d

^a*Physik-Department, Technische Universität München,
James-Frank-Strasse, D-85748 Garching, Germany*

^b*TUM Institute for Advanced Study, Technische Universität München,
Lichtenbergstrasse 2a, D-85748 Garching, Germany*

^c*Dipartimento di Fisica “G. Galilei”, Università di Padova and
INFN, Sezione di Padova, Via Marzolo 8, I-35131 Padua, Italy*

^d*Instituto de Física Teórica, IFT-UAM/CSIC,
Nicolás Cabrera 15, UAM Cantoblanco 28049, Madrid, Spain*

E-mail: luca.merlo@ph.tum.de, rigolin@pd.infn.it,
bryan.zaldivar@uam.es

ABSTRACT: We describe the phenomenology of the flavour changing neutral current sector of a supersymmetric model, invariant under the T' discrete flavour group. This model has been proposed in ref. [1] and describes realistic leptonic and hadronic masses and mixings and predicts the amount of flavour changing in terms of the small flavour breaking parameter $u \in [0.007, 0.05]$. For small values of u , the model almost reduces to the MSUGRA framework, while sizable deviations from MSUGRA can be, instead, observed when larger values of u and $\tan \beta$ are considered. We analyse in detail $T' \mu \rightarrow e\gamma$ prediction, concerning the leptonic sector, while for the hadronic sector we concentrate on $b \rightarrow s\gamma$ and neutral B meson mass differences $\Delta M_{B_{s,d}}$. Moreover, for the first time a comparative study on leptonic and hadronic observables for the T' model is performed. The experimental data on FCNC observables severely constrain the model in the small m_0 region. Conversely for larger m_0 , the T' model satisfies all the bounds.

KEYWORDS: Rare Decays, Supersymmetric Standard Model, Discrete and Finite Symmetries, Global Symmetries

ARXIV EPRINT: [1108.1795](https://arxiv.org/abs/1108.1795)

Contents

1	Introduction	1
2	General features of the supersymmetric T' model	4
3	Kinetic terms and mass matrices	8
3.1	Kähler potential	8
3.2	Superpotential	12
3.3	Sfermion masses	15
4	The physical basis	19
5	Phenomenology of the T' FCNC sector	22
5.1	SUSY mass spectrum: MSUGRA vs. T'	24
5.2	FCNC in the leptonic sector	28
5.3	FCNC in the hadronic sector	32
5.4	Cross-correlations between leptonic and hadronic observables	35
6	Conclusions	35
A	The group T'	37
B	Details on the sfermion mass matrices	38
C	Canonical normalisation of the kinetic terms and diagonalisation of $M_{\ell,d}$	44
D	Wilson coefficient contributions for $\text{BR}(\bar{B} \rightarrow X_s \gamma)$	45

1 Introduction

In the Standard Model (SM) of particle physics an explanation of the origin of the fermionic mass and mixing patterns is missing. The mass spectrum is highly hierarchical, spreading over several orders of magnitude. The quark mixing matrix V_{CKM} is close to the unity matrix and the deviations from unity are usually parametrised in powers of the (sin of the) Cabibbo angle λ :

$$V_{\text{CKM}} = \begin{pmatrix} 1 - \lambda^2/2 & \lambda & A\lambda^3(\bar{\rho} - i\bar{\eta}) \\ -\lambda & 1 - \lambda^2/2 & A\lambda^2 \\ A\lambda^3(1 - \bar{\rho} - i\bar{\eta}) & -A\lambda^2 & 1 \end{pmatrix}. \quad (1.1)$$

Recent global fits on the V_{CKM} elements [2] give the following values (at 1σ):

$$\begin{aligned} \lambda &= 0.2253 \pm 0.0007, & A &= 0.808^{+0.022}_{-0.015}, \\ \bar{\rho} &= 0.132^{+0.022}_{-0.014}, & \bar{\eta} &= 0.341 \pm 0.013. \end{aligned} \tag{1.2}$$

A fundamental theory that explains all the SM flavour parameters is missing and its search constitutes the so-called *SM flavour problem*.

While already present in the original version of the SM, the flavour problem has worsened even more after the discovery that neutrinos oscillate and consequently have both a non-vanishing mass and a non-vanishing leptonic flavour mixings. The global fit in neutrino oscillation experiments presented in ref. [2] gives the following bounds at 99.73% of C.L.:

$$\begin{aligned} 7.05 \times 10^{-5} \text{ eV}^2 &\leq \Delta m_{\text{sol}}^2 \leq 8.34 \times 10^{-5} \text{ eV}^2 \\ 2.07 \times 10^{-3} \text{ eV}^2 &\leq \Delta m_{\text{atm}}^2 \leq 2.75 \times 10^{-3} \text{ eV}^2 \end{aligned} \tag{1.3}$$

with the electron neutrino mass $m_{\nu_e} \leq 2 \text{ eV}$ from Tritium experiments [2]. Moreover the leptonic mixing matrix, U_{PMNS} has a completely different structure than the V_{CKM} , with two very large angles and the third very small. The solar, atmospheric and reactor angle (namely θ_{12} , θ_{24} and θ_{13}) bounds read (at 99.73% of C.L.):

$$\begin{aligned} 0.25 &\leq \sin^2 \theta_{12} \leq 0.37 \\ 0.36 &\leq \sin^2 \theta_{23} \leq 0.67 \\ \sin^2 \theta_{13} &\leq 0.056. \end{aligned} \tag{1.4}$$

Recently new data from T2K collaboration [3] and corresponding fits [4, 5] indicate a 3σ evidence of a non-vanishing θ_{13} with a relatively “large” central value.

A very good approximation for the lepton mixing matrix is provided by the so-called Tri-Bimaximal (TB) pattern [6–8], which corresponds to the mixing angles $\sin^2 \theta_{12}^{TB} = 1/3$, $\sin^2 \theta_{23}^{TB} = 1/2$, $\sin \theta_{13}^{TB} = 0$, and agrees at about the 1σ level with the data. The appeal of the TB scheme is also due to the independence of the mixing angles from any mass parameter: indeed they are defined only by simple numerical factors. Other mixing schemes, like the Bimaximal [9–13] and the Golden Ratio [14, 15] ones, exhibit analogous features, but the agreement with the experimental data is less promising compared to the TB one.¹

The Supersymmetric extension of the Standard Model in its most straightforward (Minimal) description (MSSM), while stabilizing the Higgs scale, severely worsens the flavour problem as order of one hundred extra parameters in the flavour sector are introduced. Most of these parameters are already highly constrained (“fine-tuned”) by present experimental data. A fundamental theory that explains the flavour mass patterns is missing in the MSSM too.

Following the idea that the fermion mass structures could arise from a symmetry principle, flavour symmetries have been introduced, both in the context of the SM and its supersymmetric (SUSY) extensions. However a commonly accepted approach is still missing and many different examples have been proposed in the literature based on a large variety of symmetries: either abelian or non-abelian, local or global, continuous or discrete.

¹Typical TB models predict $\sin^2 \theta_{13} \approx 0.003$ with a tension with the present T2K central value: $\sin^2 \theta_{13} = 0.029$.

The largest flavour symmetry allowed in the SM in the limit of vanishing Yukawas couplings is $U(3)^5$, i.e. the symmetry of the kinetic terms. Such a symmetry is implemented in the so-called Minimal Flavour Violation (MFV) ansatz [16–19]: a very concise and predictive framework built on the assumption that, at low energy, the Yukawa couplings are the only sources of flavour and CP violation both in the SM and in any possible extension beyond it. The technical realisation of the MFV ansatz promotes the Yukawa matrices to *spurion* fields, thus making the Lagrangian manifestly invariant under the full flavour symmetry. Any model beyond the SM, implemented with the MFV ansatz, is successful in suppressing flavour changing neutral current (FCNC) contributions with a typical new physics flavour scale in the TeV region. When the symmetry is gauged [20–22], new effects could arise as it has been recently pointed out in [23].

On the other hand, a natural mechanism to explain fermions masses and mixings in the MFV framework is still missing [24, 25]. Some improvements in this direction are possible when considering smaller symmetry groups. However, any deviation from the MFV scheme, usually allows the appearance of dangerous flavour violating contributions. Interesting attempts, in which FCNC processes are under control and the fermion mass origin is discussed, are the one adopting as continuous symmetries $U(2)$ [26–28], $U(2)^3$ [29, 30], $SU(3)$ and $SO(3)$ [31–35]. Notice that only in refs. [31–35] both the fermion sectors are fully discussed; however, in such papers, an *ad hoc* dynamics is adopted to achieve the Yukawa textures.

Discrete symmetries represent an alternative solution to the flavour problem, exhibiting their power especially in the leptonic sector. In [36–40] it has been pointed out that a (spontaneously broken) flavour symmetry based on the discrete group A_4 appears to be particularly suitable to reproduce the TB lepton mixing pattern as a first approximation. Many other solutions have also been considered to generate the TB scheme, based on larger discrete flavour groups,² such as S_4 , T' and $\Delta(27)$. Discrete symmetries have been successfully used to describe also the Bimaximal [42, 43] and the Golden Ratio [44, 45] schemes.

Models based on discrete symmetries, however, usually highly deviate from the MFV framework and potentially large flavour violating contributions are expected. In spite of the large effort devoted in describing flavour models predicting mass patterns in agreement with the data, only few studies analysed possible contributions to lepton flavour violating (LFV) and FCNC observables [46–55]. In particular, the phenomenology of the Altarelli-Feruglio (AF) lepton model [38–40], based on A_4 , has been studied in details both in the SM [56, 57] and in the SUSY [58–61] scenario. The main result of these analyses is that the flavour symmetry not only governs the structure of the fermion masses and mixings, but also constrains the relative contribution to flavour violating observables, such as for example the $\ell_i \rightarrow \ell_j \gamma$ decays. In this context, in fact, the predicted rates of FCNC processes are more suppressed than in a general effective operator approach [62], due to peculiar cancellations, allowing for a new physics scale close to the TeV range, without conflicting with the present bounds. This type of analysis is therefore essential for testing a specific model and for providing predictions which could allow to discriminate among all the available proposals.

²As a review on the possible discrete groups see for example [41].

	ℓ	e^c	μ^c	τ^c	D_q	D_u^c	D_d^c	q_3	t^c	b^c	$H_{u,d}$
T'	3	1	1''	1'	2''	2''	2''	1	1	1	1
Z_3	ω	ω^2	ω^2	ω^2	ω	ω^2	ω^2	ω	ω^2	ω^2	1
$U(1)_{\text{FN}}$	0	2	1	0	0	1	1	0	0	1	0
$U(1)_{\text{R}}$	1	1	1	1	1	1	1	1	1	1	0

Table 1. The transformation properties of matter fields and Higgses under the flavour group G_f .

In ref. [1] a SUSY model based on the discrete group T' has been constructed. This model accounts both for leptons, predicting the TB mixing pattern, and for quarks, providing a realistic CKM matrix. In particular, the lepton sector corresponds to that of the AF model and therefore this T' model can be considered as an extension of the SUSY AF model to the quark sector. However in ref. [1] no phenomenological analysis of the hadronic sector has been presented. Consequently, the main goal of the present paper is to fill this gap and to present a complete description of FCNC observables both for leptons and hadrons.

The paper is organized as follows: in section 2 the general features of the T' model are briefly reminded. In section 3 the kinetic terms and the mass matrices for fermions and sfermions are derived in a particularly convenient basis, and then in section 4 the results are presented in a more “physical” basis. Most of the details regarding the derivation of the soft mass matrices and the connection between the two basis are deferred to the appendices. The main phenomenological results of the T' model are described in section 5. Finally we conclude in section 6.

2 General features of the supersymmetric T' model

The T' model, we are interested in, has been proposed in ref. [1]. We summarise here the notation and the main results, pointing out, when necessary, the few slight differences introduced here.

The full flavour group, G_f , is a product of various terms,

$$G_f = T' \times Z_3 \times U(1)_{\text{FN}} \times U(1)_{\text{R}}, \tag{2.1}$$

each of them playing a different role. The spontaneous breaking of the T' group (see appendix A and ref. [1]) is mainly responsible for the fermion mixings, while the correct fermion mass hierarchies mainly originate from a combined effect of the Z_3 and $U(1)_{\text{FN}}$ groups. Indeed the Z_3 symmetry is used to forbid unwanted couplings between the SM fields and the extra fields added in the model that will be specified in the following; the continuous $U(1)_{\text{FN}}$ provides, according to the original Froggatt-Nielsen mechanism [63], the suppressions necessary to reproduce the mass hierarchies. Finally, the $U(1)_{\text{R}}$ is a common ingredient of SUSY constructions, containing the usual R -parity as a subgroup.

The matter fields of the model, together with their transformation properties under the flavour group, are listed in table 1 adopting, both for fields and their superpartners, the following notation: $\ell = (\ell_1, \ell_2, \ell_3)$, where $\ell_1 = (\nu_e, e)$, $\ell_2 = (\nu_\mu, \mu)$ and $\ell_3 = (\nu_\tau, \tau)$,

	θ	φ_T	φ_S	$\xi, \tilde{\xi}$	η	ξ''
T'	$\mathbf{1}$	$\mathbf{3}$	$\mathbf{3}$	$\mathbf{1}$	$\mathbf{2}'$	$\mathbf{1}''$
Z_3	1	1	ω	ω	1	1
$U(1)_{\text{FN}}$	-1	0	0	0	0	0
$U(1)_{\text{R}}$	0	0	0	0	0	0

Table 2. The transformation properties of flavon fields under the flavour group G_f .

are the $SU(2)_L$ -doublet (s)leptons; e^c, μ^c and τ^c are the $SU(2)_L$ -singlet (s)leptons; $D_q = (q_1, q_2)$, where $q_1 = (u, d)$ and $q_2 = (c, s)$, are the $SU(2)_L$ -doublet (s)quarks of the first two generations; $D_u^c = (u^c, c^c)$ and $D_d^c = (d^c, s^c)$ are the $SU(2)_L$ -singlet (s)quarks of the first two generations; $q_3 = (t, b)$ is the $SU(2)_L$ -doublet (s)quark of the third generation while t^c and b^c are the $SU(2)$ -singlet (s)quarks of the third generation. $H_{u,d}$ are the two usual SUSY Higgs doublets. Under the discrete symmetry group T' , ℓ transforms as a triplet, D_q, D_u^c and D_d^c as doublets, $e^c, \mu^c, \tau^c, q_3, t^c, b^c$ and $H_{u,d}$ are singlets.

Apart from matter superfields the spectrum of the model accounts for several scalar fields that are neutral under the SM gauge group. Their transformation properties under the flavour group G_f are shown in table 2. This new set of scalar fields is responsible for the spontaneous breaking of the flavour symmetry and are usually called *flavons*. As described in details in [1], it is possible to construct a scalar potential in such a way that flavons develop vacuum expectation values (vevs) along the following (flavour) directions:

$$\begin{aligned}
 \frac{\langle \varphi_T \rangle}{\Lambda_f} &= (u, 0, 0) + (c_{T1} u^2, c_{T2} t u^2, c_{T3} u^2), \\
 \frac{\langle \varphi_S \rangle}{\Lambda_f} &= c_b (u, u, u) + \mathcal{O}(u^2), \\
 \frac{\langle \eta \rangle}{\Lambda_f} &= c' (u, 0) + (c_{\eta 1} u^2, c_{\eta 2} u^2), \\
 \frac{\langle \xi \rangle}{\Lambda_f} &= c_a u + \mathcal{O}(u^2), \quad \frac{\langle \tilde{\xi} \rangle}{\Lambda_f} = c_c u^2, \quad \frac{\langle \xi'' \rangle}{\Lambda_f} = c'' u^2, \quad \frac{\langle \theta_{\text{FN}} \rangle}{\Lambda_f} = t.
 \end{aligned}
 \tag{2.2}$$

All the coefficients c_i , appearing in eqs. (2.2), are complex numbers with absolute value of order one, while u and t are two, small, T' symmetry breaking parameters. In eqs. (2.2) we explicitly considered all contributions up to second order in u , when relevant. Notice that both u and t can, in general, be complex, but one can show that, through fields redefinitions, they can be taken real and positive. The cutoff scale Λ_f is associated to the flavour dynamics and it is expected close to the grand unification scale, $\Lambda_f \lesssim 10^{16}$ GeV.

In ref. [1] the most general superpotential invariant under the SM gauge group and under G_f has been constructed, according to the transformation properties listed in tables 1 and 2. Considering only the leading-order (LO) terms in the u expansion of such a superpotential and the corresponding LO approximation of the expressions in eq. (2.2), the charged leptons mass matrix reads:

$$M_\ell \propto \begin{pmatrix} y_e t^2 & 0 & 0 \\ 0 & y_\mu t & 0 \\ 0 & 0 & y_\tau \end{pmatrix} u, \tag{2.3}$$

with y_e, y_μ and y_τ being complex numbers with absolute values of order one. The parameter t governs the relative hierarchy among the charged lepton masses. Through a comparison with the experimental data one infers $t \approx 0.05$. A lower bound on u can be obtained from the relation that connects the T' breaking parameter to the SM electroweak vev (v), the τ Yukawa coupling and pole mass (y_τ and m_τ) and the MSSM neutral Higgs vevs. ratio ($\tan \beta = v_u/v_d$):

$$u = \frac{1}{|y_\tau|} \frac{\sqrt{2} m_\tau}{v \cos \beta} \approx 0.01 \frac{\tan \beta}{|y_\tau|}. \quad (2.4)$$

By requiring a τ -Yukawa coupling consistent with the perturbative regime, $|y_\tau| < 3$, one gets $u \geq 0.05$ (0.007) for $\tan \beta = 15$ (2) respectively.

Following ref. [1], at the LO the light neutrino mass matrix is given by

$$M_\nu \propto \begin{pmatrix} 3a + 2b & -b & -b \\ -b & 2b & 3a - b \\ -b & 3a - b & 2b \end{pmatrix} u, \quad (2.5)$$

and it can be diagonalised by the TB mixing matrix, defined, up to phases, by

$$U_{TB} = \begin{pmatrix} \sqrt{2/3} & 1/\sqrt{3} & 0 \\ -1/\sqrt{6} & 1/\sqrt{3} & -1/\sqrt{2} \\ -1/\sqrt{6} & 1/\sqrt{3} & +1/\sqrt{2} \end{pmatrix}. \quad (2.6)$$

When considering the sub-leading contributions to the matter superpotential in the u expansion (see ref. [1] for details) and the corresponding sub-leading terms in eq. (2.2), the mass matrices in eqs. (2.3) and (2.5) get modified and consequently the diagonalisation matrix in eq. (2.6) slightly deviates from the TB pattern. An upper bound on u of about 0.05 is obtained by the requirement that these corrections do not perturb excessively the TB values of the neutrino mixing angles: the strongest constraint provided by the solar mixing angle. As a consequence, for $\tan \beta = 2$ only values for u in the range

$$0.007 \lesssim u \lesssim 0.05 \quad (2.7)$$

are allowed, while for $\tan \beta = 15$ only $u = 0.05$ is permitted.

Considering the quark sector, the particular choice of the transformation properties for the quark fields and the specific alignment of the flavon vevs. determine the characteristic “shell” filling of the mass matrices. In terms of the T' breaking parameters u and t , they read:

$$M_u \sim \begin{pmatrix} t^2 u^2 & t u^2 & t u^2 \\ t u^2 & t u & t u \\ u^2 & u & 1 \end{pmatrix}, \quad M_d \sim \begin{pmatrix} t^2 u^2 & \sqrt{t} u^2 & t u^2 \\ \sqrt{t} u^2 & t u & t u \\ t u^2 & t u & t \end{pmatrix}. \quad (2.8)$$

In the previous mass matrices we didn't explicitly write the unknown, order one, coefficients entering in each of the entries. In the largest part of the allowed range for u , realistic quark masses and CKM mixings follow from eqs. (2.8). Only when very small values for u are

Field	φ_T^0	φ_S^0	η^0	ξ^0	ξ'^0
T'	3	3	2''	1	1'
Z_3	1	ω	1	ω	1
$U(1)_{\text{FN}}$	0	0	0	0	0
$U(1)_{\text{R}}$	2	2	2	2	2

Table 3. The transformation properties of the driving fields under the flavour group G_f .

considered, it is necessary to compensate with coefficients slightly larger than one. We will discuss this issue more in detail in the following sections.

In order to break the flavour group along the required directions and to allow the flavons to get vevs. as in eqs. (2.2), a new set of fields, called *driving* superfields, has to be introduced. These fields transform only under the flavour group G_f and couple only to the flavons. The driving fields, together with their transformation properties under G_f , are listed in table 3.

As it has been discussed in [58, 60], in the context of the A_4 model, the driving fields develop non-vanishing vevs. only once soft SUSY breaking terms are introduced. Extending such an analysis to the case of the T' model, the following vevs. for the driving superfields are obtained: to first order in u they are given by

$$\begin{aligned}
 \frac{\langle \varphi_T^0 \rangle}{m_0} &= c_T^0(1, 0, 0) + (c_{T1}^0 u, c_{T2}^0 u, c_{T3}^0 u), \\
 \frac{\langle \varphi_S^0 \rangle}{m_0} &= c_b^0(1, 1, 1) + (c_{S1}^0 u, c_{S2}^0 u, c_{S3}^0 u), \\
 \frac{\langle \eta^0 \rangle}{m_0} &= (0, c_\eta^0) + (c_{\eta1}^0 u, c_{\eta2}^0 u), \\
 \frac{\langle \xi^0 \rangle}{m_0} &= c_a^0 + c_c^0 u, \quad \frac{\langle \xi'^0 \rangle}{m_0} = c_{\xi'}^0 u.
 \end{aligned}
 \tag{2.9}$$

All the coefficients c_i^0 , appearing in the previous equations, are complex numbers with absolute value of order one. Here, m_0 represents the common soft SUSY breaking scalar mass. Starting from eqs. (2.2) and (2.9), the vevs. of the flavon F -terms which non-trivially contribute to the sfermion mass matrices can be derived:

$$\begin{aligned}
 \frac{1}{\Lambda_f} \left\langle \frac{\partial w}{\partial \varphi_T} \right\rangle &= m_0 [c^F(u, 0, 0) + (c_{T1}^F u^2, c_{T2}^F u^2, c_{T3}^F u^2)], \\
 \frac{1}{\Lambda_f} \left\langle \frac{\partial w}{\partial \varphi_S} \right\rangle &= m_0 [c_b^F(u, u, u) + (c_{S1}^F u^2, c_{S2}^F u^2, c_{S3}^F u^2)], \\
 \frac{1}{\Lambda_f} \left\langle \frac{\partial w}{\partial \eta} \right\rangle &= m_0 [c^{F'}(u, 0) + (c_{\eta1}^F u^2, c_{\eta2}^F u^2)], \\
 \frac{1}{\Lambda_f} \left\langle \frac{\partial w}{\partial \xi} \right\rangle &= m_0 c_a^F u, \quad \frac{1}{\Lambda_f} \left\langle \frac{\partial w}{\partial \tilde{\xi}} \right\rangle = m_0 c_c^F u^2, \quad \frac{1}{\Lambda_f} \left\langle \frac{\partial w}{\partial \xi''} \right\rangle = m_0 c^{F''} u^2.
 \end{aligned}
 \tag{2.10}$$

Again all the coefficients c_i^F are complex numbers with absolute value of order one. It is interesting to note that the LO terms in eq. (2.10) are proportional to those in eq. (2.2), confirming what found in [1, 58, 64].

3 Kinetic terms and mass matrices

The Lagrangian of the SUSY T' model from which both fermion and sfermion masses are obtained, is given by

$$\mathcal{L} = \int d^2\theta d^2\bar{\theta} \mathcal{K}(\bar{z}, e^{2V} z) + \left[\int d^2\theta w(z) + \text{h.c.} \right] + \frac{1}{4} \left[\int d^2\theta f(z) \mathcal{W} \mathcal{W} + \text{h.c.} \right], \quad (3.1)$$

where $\mathcal{K}(\bar{z}, z)$ is the Kähler potential, $w(z)$ is the superpotential and $f(z)$ is the gauge kinetic function. V is the Lie-algebra valued vector supermultiplet, describing the gauge fields and their superpartners while \mathcal{W} is the chiral superfield describing, together with the function $f(z)$, the kinetic terms of gauge bosons and their superpartners. Notice that the fermion sector has already been discussed in ref. [1], but assuming canonical kinetic terms.

It is assumed that the breaking of SUSY occurs at a scale higher than or comparable to the flavour scale, so that at energies close to the cutoff scale we have non-universal boundary conditions for the soft SUSY breaking terms, dictated by the flavour symmetry. The soft SUSY breaking terms are generated from the SUSY Lagrangian by promoting all coupling constants (such as the Yukawa couplings, the couplings in the flavon superpotential and the couplings in the Kähler potential) to superfields with constant θ^2 and $\theta^2\bar{\theta}^2$ components [65]. The analysis of the lepton sector is going to be the same as the one presented in ref. [60] for the AF model, but for the presence in the T' case of two additional flavons: η and ξ'' .

3.1 Kähler potential

For non-vanishing values of the T' breaking parameters u and t , the Kähler potential deviates from the canonical form, $\mathcal{K}(\bar{z}, z) = \bar{z}z$, due to the contributions of non-renormalizable terms, invariant under both the gauge and the flavour symmetries, containing the flavon fields. Such terms are suitably suppressed by the flavour scale Λ_f , but cannot be neglected as they affect the fermionic mass matrices, through redefinitions needed to move into the basis of canonically normalised kinetic terms. In the following we are going to include all the terms up to the second order in the expansion in u and additional contributions proportional to t , when needed in order not to have vanishing elements in the sfermion mass matrices.

The Kähler potential can be written as $\mathcal{K} = \mathcal{K}_\ell + \mathcal{K}_q + \mathcal{K}_r$ where the three terms correspond to lepton, quark and remaining field contributions, respectively. Let us start considering the leptonic contribution:

$$\mathcal{K}_\ell = \mathcal{K}_\ell^{(0)} + \mathcal{K}_\ell^{(1)} + \mathcal{K}_\ell^{(2)} + \dots \quad (3.2)$$

where $\mathcal{K}_\ell^{(i)}$ represents the i^{th} term in the u expansion. The LO term reads:

$$\mathcal{K}_\ell^{(0)} = k_0^\ell \sum_{i=1}^3 \bar{\ell}_i \ell_i + \sum_{i=1}^3 \left[(k_0^e)_i + (\hat{k}_0^e)_i \frac{|\theta_{\text{FN}}|^2}{\Lambda_f^2} \right] \bar{\ell}_i^c \ell_i^c \quad (3.3)$$

with $\ell^c = (e^c, \mu^c, \tau^c)$. Notice that the contributions from the superfield θ_{FN} can be neglected, with the exception of the right-handed sector, where we consider terms up to second order in t . The next order term in the u expansion is given by

$$\begin{aligned} \mathcal{K}_\ell^{(1)} = & \frac{k_S^\ell}{\Lambda_f} (\varphi_T(\bar{\ell}\ell)_S) + \frac{k_A^\ell}{\Lambda_f} (\varphi_T(\bar{\ell}\ell)_A) + \frac{k_{\xi''}^\ell}{\Lambda_f} \xi''(\bar{\ell}\ell)' + \\ & + \frac{k_S^{\ell'}}{\Lambda_f} (\bar{\varphi}_T(\bar{\ell}\ell)_S) + \frac{k_A^{\ell'}}{\Lambda_f} (\bar{\varphi}_T(\bar{\ell}\ell)_A) + \frac{k_{\xi''}^{\ell'}}{\Lambda_f} \xi''(\bar{\ell}\ell)'' + \text{h.c.} \end{aligned} \quad (3.4)$$

where (\dots) , $(\dots)'$ and $(\dots)''$ denote the $\mathbf{1}$, $\mathbf{1}'$ and $\mathbf{1}''$ singlets of T' , while $(\dots)_S$ and $(\dots)_A$ the symmetric and antisymmetric triplets originating from the contraction of two $\mathbf{3}$ representations (see the appendix A for details). Notice that the $\text{SU}(2)_L$ singlet superfields ℓ^c are not affected at this order in the expansion. To discuss the next term it is useful to distinguish the contributions to the left-handed doublets and the right-handed singlets:

$$\mathcal{K}_\ell^{(2)} = \mathcal{K}_{\ell L}^{(2)} + \mathcal{K}_{\ell R}^{(2)}. \quad (3.5)$$

For lepton doublets one finds:

$$\mathcal{K}_{\ell L}^{(2)} = \sum_{i=1}^{17} \frac{k_i^\ell}{\Lambda_f^2} (X_i^\ell \bar{\ell}\ell) \quad (3.6)$$

where X^ℓ is a list of Z_3 -invariant operators, bilinear in the flavon superfields and their conjugates,

$$\begin{aligned} X^\ell = & \left\{ \bar{\xi}\xi, \varphi_T^2, \bar{\varphi}_T^2, \bar{\varphi}_T\varphi_T, \bar{\varphi}_S\varphi_S, \bar{\xi}''\xi'', \bar{\eta}\eta, \bar{\xi}\varphi_S, \bar{\varphi}_S\xi, \right. \\ & \left. \xi''^2, \bar{\xi}''^2, \eta^2, \bar{\eta}^2, \varphi_T\xi'', \bar{\varphi}_T\xi'', \varphi_T\bar{\xi}'', \bar{\varphi}_T\bar{\xi}'' \right\}, \end{aligned} \quad (3.7)$$

and each quantity k_i^ℓ represents a list of parameters since there can be different non-equivalent ways of combining X_i^ℓ with $\bar{\ell}\ell$ to form a T' -invariant. There are also obvious relations among the coefficients k_i^ℓ to guarantee that $\mathcal{K}_{\ell L}^{(2)}$ is real. Notice that in X^ℓ we do not consider the possible combinations with the flavon ξ , because it has exactly the same quantum numbers as ξ and therefore their contributions can be identified by the same coupling constant. Furthermore, notice that some of the terms in the sum of eq. (3.6) are vanishing once we consider specific vevs. of the flavons in eq. (2.2).

For lepton singlets, we can distinguish a diagonal contribution and a non-diagonal one:

$$\mathcal{K}_{\ell R}^{(2)} = \left[\mathcal{K}_{\ell R}^{(2)} \right]_{\text{d}} + \left[\mathcal{K}_{\ell R}^{(2)} \right]_{\text{nd}}$$

respectively given by:

$$\left[\mathcal{K}_{\ell R}^{(2)}\right]_d = \frac{1}{\Lambda_f^2} \sum_{i=1}^7 \left[(k_e^e)_i (X_i^\ell) \bar{e}^c e^c + (k_\mu^e)_i (X_i^\ell) \bar{\mu}^c \mu^c + (k_\tau^e)_i (X_i^\ell) \bar{\tau}^c \tau^c \right], \quad (3.8)$$

$$\begin{aligned} \left[\mathcal{K}_{\ell R}^{(2)}\right]_{\text{nd}} &= \frac{\bar{\theta}_{\text{FN}}}{\Lambda_f^2} (k_{e\mu}^e)_1 \bar{\xi}'' \bar{e}^c \mu^c + \frac{\bar{\theta}_{\text{FN}}^2}{\Lambda_f^3} (k_{e\tau}^e)_1 \xi'' \bar{e}^c \tau^c + \frac{\bar{\theta}_{\text{FN}}}{\Lambda_f^2} (k_{\mu\tau}^e)_1 \bar{\xi}'' \bar{\mu}^c \tau^c + \\ &+ \frac{\bar{\theta}_{\text{FN}}}{\Lambda_f^3} \left[\sum_{i=2}^5 (k_{e\mu}^e)_i (X_i^\ell)' + (k_{e\mu}^e)_6 X_{10}^\ell + (k_{e\mu}^e)_7 X_{13}^\ell \right] \bar{e}^c \mu^c + \\ &+ \frac{\bar{\theta}_{\text{FN}}^2}{\Lambda_f^4} \left[\sum_{i=2}^5 (k_{e\tau}^e)_i (X_i^\ell)'' + (k_{e\tau}^e)_6 X_{11}^\ell + (k_{e\tau}^e)_7 X_{12}^\ell \right] \bar{e}^c \tau^c + \\ &+ \frac{\bar{\theta}_{\text{FN}}}{\Lambda_f^3} \left[\sum_{i=2}^5 (k_{\mu\tau}^e)_i (X_i^\ell)' + (k_{\mu\tau}^e)_6 X_{10}^\ell + (k_{\mu\tau}^e)_7 X_{13}^\ell \right] \bar{\mu}^c \tau^c + \text{h.c.} . \end{aligned} \quad (3.9)$$

Due to the structure of the flavon vevs. at LO, the first row in eq. (3.9) vanish. If also the next-to-leading order (NLO) is considered, these terms contribute at the same level as the operators in the subsequent rows. The expressions in eqs. (3.3)–(3.9) reduce to the ones of [60] when the contributions related to the flavons η and ξ'' are singled out.

The same expansion in u can be considered similarly for the Kähler potential of the quark sector, \mathcal{K}_q :

$$\mathcal{K}_q = \mathcal{K}_q^{(0)} + \mathcal{K}_q^{(1)} + \mathcal{K}_q^{(2)} + \dots \quad (3.10)$$

The LO terms in the u expansion are given by:

$$\begin{aligned} \mathcal{K}_q^{(0)} &= k_0^Q \sum_{i=1}^2 \bar{D}_{q_i} D_{q_i} + \left[k_0^{q_3} + \hat{k}_0^{q_3} \frac{|\theta_{\text{FN}}|^2}{\Lambda_f} \right] \bar{q}_3 q_3 + \\ &+ k_0^U \sum_{i=1}^2 \bar{D}_{u_i}^c D_{u_i}^c + \left[k_0^t + \hat{k}_0^t \frac{|\theta_{\text{FN}}|^2}{\Lambda_f} \right] \bar{t}^c t^c + \\ &+ k_0^D \sum_{i=1}^2 \bar{D}_{d_i}^c D_{d_i}^c + \left[k_0^b + \hat{k}_0^b \frac{|\theta_{\text{FN}}|^2}{\Lambda_f} \right] \bar{b}^c b^c . \end{aligned} \quad (3.11)$$

Notice again that the contributions from the superfield θ_{FN} can be neglected, with the exception of the third families, where we consider terms up to second order in t . The next terms in the u expansion are given by:

$$\begin{aligned} \mathcal{K}_q^{(1)} &= \frac{k_T^Q}{\Lambda_f} (\varphi_T (\bar{D}_q D_q)_3) + \frac{k_T^{Q'}}{\Lambda_f} (\bar{\varphi}_T (\bar{D}_q D_q)_3) + \frac{k_\eta^Q}{\Lambda_f} (\bar{\eta} \bar{D}_q) q_3 + \\ &+ \frac{k_T^U}{\Lambda_f} (\varphi_T (\bar{D}_u^c D_u^c)_3) + \frac{k_T^{U'}}{\Lambda_f} (\bar{\varphi}_T (\bar{D}_u^c D_u^c)_3) + \frac{k_\eta^U}{\Lambda_f^2} \bar{\theta}_{\text{FN}} (\bar{\eta} \bar{D}_u^c) t^c + \\ &+ \frac{k_T^D}{\Lambda_f} (\varphi_T (\bar{D}_d^c D_d^c)_3) + \frac{k_T^{D'}}{\Lambda_f} (\bar{\varphi}_T (\bar{D}_d^c D_d^c)_3) + \frac{k_\eta^D}{\Lambda_f} (\bar{\eta} \bar{D}_d^c) b^c + \text{h.c.} \end{aligned} \quad (3.12)$$

$$\begin{aligned}
 \mathcal{K}_q^{(2)} = & \sum_{i=1}^{15} \frac{k_i^Q}{\Lambda_f^2} (X_i^q \bar{D}_q D_q) + \sum_{i=1}^7 \frac{k_i^{q3}}{\Lambda_f^2} (X_i^q) \bar{q}_3 q_3 + \sum_{i=1}^5 \frac{k_i^{Qq3}}{\Lambda_f^2} (X_{i+15}^q \bar{D}_q) q_3 + \\
 & + \sum_{i=1}^{15} \frac{k_i^U}{\Lambda_f^2} (X_i^q \bar{D}_u D_u^c) + \sum_{i=1}^7 \frac{k_i^t}{\Lambda_f^2} (X_i^q) \bar{t}^c t^c + \sum_{i=1}^5 \frac{k_i^{Ut}}{\Lambda_f^3} \bar{\theta}_{\text{FN}} (X_{i+15}^q \bar{D}_u^c) t^c + \\
 & + \sum_{i=1}^{15} \frac{k_i^D}{\Lambda_f^2} (X_i^q \bar{D}_d D_d^c) + \sum_{i=1}^7 \frac{k_i^b}{\Lambda_f^2} (X_i^q) \bar{b}^c b^c + \sum_{i=1}^5 \frac{k_i^{Db}}{\Lambda_f^2} (X_{i+15}^q \bar{D}_d^c) b^c + \text{h.c.}
 \end{aligned} \tag{3.13}$$

where X^q is a list of Z_3 -invariant operators, bilinear in the flavon superfields and their conjugates,

$$\begin{aligned}
 X^q = & \left\{ \bar{\xi} \xi, \varphi_T^2, (\bar{\varphi}_T)^2, \bar{\varphi}_T \varphi_T, \bar{\varphi}_S \varphi_S, \bar{\xi}'' \xi'', \bar{\eta} \eta, \bar{\xi} \varphi_S, \bar{\varphi}_S \xi, \varphi_T \xi'', \bar{\varphi}_T \xi'', \right. \\
 & \left. \varphi_T \bar{\xi}'', \bar{\varphi}_T \bar{\xi}'', \eta^2, \bar{\eta}^2, \bar{\xi}'' \eta, \varphi_T \eta, \bar{\varphi}_T \eta, \varphi_T \bar{\eta}, \bar{\varphi}_T \bar{\eta} \right\},
 \end{aligned} \tag{3.14}$$

and each k_i represents a list of parameters since there can be different non-equivalent ways of combining X_i^q to quark superfields to form a T' -invariant. There are also obvious relations among the coefficients k_i in order to guarantee the realness of $\mathcal{K}_{qL}^{(2)}$. For the same reason as for X^ℓ , also in this case we do not consider in X^q the possible combinations with the flavon $\tilde{\xi}$.

Finally, the Kähler potential containing the Higgs and FN fields is given by:

$$\mathcal{K}_r = k_u |H_u|^2 + k_d |H_d|^2 + k_{\text{FN}} |\theta_{\text{FN}}|^2 + \dots \tag{3.15}$$

where dots stand for additional contributions related to the flavon sector.

In order to generate a set of SUSY breaking soft mass terms, each coupling constant k_I is treated as a superfield with non-vanishing constant $\theta^2 \bar{\theta}^2$ component:

$$k_I = p_I + s_I \theta^2 \bar{\theta}^2 m_0^2 \tag{3.16}$$

where p_I and s_I are complex numbers with absolute value of order one. A more general expression could be considered, including also terms proportional to θ^2 and to $\bar{\theta}^2$ [65], but these contributions can be absorbed by a suitable reparametrisation. In the following analysis it is useful to choose a simplified notation for some of the k parameters:

$$\begin{aligned}
 k_0^\ell &= 1 + s_0^\ell \theta^2 \bar{\theta}^2 m_0^2, & (k_0^e)_i &= 1 + (s_0^e)_i \theta^2 \bar{\theta}^2 m_0^2, \\
 k_{u,d} &= 1 + s_{u,d} \theta^2 \bar{\theta}^2 m_0^2, & k_{\text{FN}} &= 1 + s_{\text{FN}} \theta^2 \bar{\theta}^2 m_0^2.
 \end{aligned} \tag{3.17}$$

When the flavons develop vevs, the Kähler potential gives rise to non-canonical kinetic terms:

$$\begin{aligned}
 \mathcal{L}_{\text{kin}} = & i K_{ij}^\ell \bar{\ell}_i \bar{\sigma}^\mu \mathcal{D}_\mu \ell_j + i K_{ij}^e \bar{\ell}_i^c \bar{\sigma}^\mu \mathcal{D}_\mu \ell_j^c + \\
 & + i K_{ij}^q \bar{Q}_i \bar{\sigma}^\mu \mathcal{D}_\mu Q_j + i K_{ij}^u \bar{U}_i^c \bar{\sigma}^\mu \mathcal{D}_\mu U_j^c + i K_{ij}^d \bar{D}_i^c \bar{\sigma}^\mu \mathcal{D}_\mu D_j^c + \\
 & + K_{ij}^\ell \overline{\mathcal{D}^\mu \bar{\ell}_i} \mathcal{D}_\mu \tilde{\ell}_j + K_{ij}^e \overline{\mathcal{D}^\mu \bar{\ell}_i^c} \mathcal{D}_\mu \tilde{\ell}_j^c + \\
 & + K_{ij}^q \overline{\mathcal{D}^\mu \bar{Q}_i} \mathcal{D}_\mu \tilde{Q}_j + K_{ij}^u \overline{\mathcal{D}^\mu \bar{U}_i^c} \mathcal{D}_\mu \tilde{U}_j^c + K_{ij}^d \overline{\mathcal{D}^\mu \bar{D}_i^c} \mathcal{D}_\mu \tilde{D}_j^c,
 \end{aligned} \tag{3.18}$$

with $Q \equiv \{q_1, q_2, q_3\}$, $U^c \equiv \{u^c, c^c, t^c\}$, $D^c \equiv \{d^c, s^c, b^c\}$, and the matrices K^i given by

$$K^\ell = \begin{pmatrix} 1 + 2t_1^\ell u & t_4^\ell u^2 & t_5^\ell u^2 \\ \bar{t}_4^\ell u^2 & 1 - (t_1^\ell + t_2^\ell) u & t_6^\ell u^2 \\ \bar{t}_5^\ell u^2 & \bar{t}_6^\ell u^2 & 1 - (t_1^\ell - t_2^\ell) u \end{pmatrix}, \quad (3.19)$$

$$K^e = \begin{pmatrix} 1 + t_1^e u^2 + t_1^{\prime e} t^2 & t_4^e u^2 t & t_5^e u^2 t^2 \\ \bar{t}_4^e u^2 t & 1 + t_2^e u^2 + t_2^{\prime e} t^2 & t_6^e u^2 t \\ \bar{t}_5^e u^2 t^2 & \bar{t}_6^e u^2 t & 1 + t_3^e u^2 + t_3^{\prime e} t^2 \end{pmatrix}, \quad (3.20)$$

$$K^q = \begin{pmatrix} t_d^q - t_1^q u & t_5^q u^2 & t_6^q u^2 \\ \bar{t}_5^q u^2 & t_d^q + t_1^q u & t_4^q u \\ \bar{t}_6^q u^2 & \bar{t}_4^q u & t_s^q + t_2^q u^2 + t_3^q t^2 \end{pmatrix}, \quad (3.21)$$

$$K^u = \begin{pmatrix} t_d^u - t_1^u u & t_5^u u^2 & t_6^u u^2 t \\ \bar{t}_5^u u^2 & t_d^u + t_1^u u & t_4^u u t \\ \bar{t}_6^u u^2 t & \bar{t}_4^u u t & t_s^u + t_2^u u^2 + t_3^u t^2 \end{pmatrix}, \quad (3.22)$$

$$K^d = \begin{pmatrix} t_d^d - t_1^d u & t_5^d u^2 & t_6^d u^2 \\ \bar{t}_5^d u^2 & t_d^d + t_1^d u & t_4^d u \\ \bar{t}_6^d u^2 & \bar{t}_4^d u & t_s^d + t_2^d u^2 + t_3^d t^2 \end{pmatrix}. \quad (3.23)$$

All these coefficients are complex, apart from $t_{1,2}^\ell$, $t_{1,2,3}^e$, $t_{1,2,3}^{\prime e}$ and $t_{d,s,1,2,3}^{q,u,d}$ that are real. Furthermore, all the t_I parameters are linearly related to the parameters p_I introduced before in eq. (3.16), but such relations are not particularly significant and in the rest of this paper we will treat the t_I coefficients as input parameters. Notice that K^ℓ and K^e have exactly the same structure of the corresponding matrices in ref. [60]. The only difference from ref. [60] is hidden in different relations between the parameters t_I and p_I in the matrices K^ℓ and K^e , due to the presence of the flavons η and ξ'' . The matrices for the quark sector are, instead, derived for the first time and extend the analysis presented in ref. [60].

3.2 Superpotential

As for the Kähler potential, also the superpotential can be separated in several parts:

$$w = w_\ell + w_\nu + w_q + w_d + w_h + \dots \quad (3.24)$$

representing respectively the charged lepton, the neutrino, the quark, the driving field and the Higgs terms. Again, each term can be written as an expansion, up to the second order, in the parameter u .

The part responsible for the charged lepton masses has a LO and NLO terms:

$$w_\ell = w_\ell^{(1)} + w_\ell^{(2)} + \dots, \quad (3.25)$$

respectively given by

$$w_\ell^{(1)} = \frac{x_e}{\Lambda_f} \frac{\theta_{\text{FN}}^2}{\Lambda_f^2} e^c H_d (\varphi_T \ell) + \frac{x_\mu}{\Lambda_f} \frac{\theta_{\text{FN}}}{\Lambda_f} \mu^c H_d (\varphi_T \ell)' + \frac{x_\tau}{\Lambda_f} \tau^c H_d (\varphi_T \ell)'' , \quad (3.26)$$

$$\begin{aligned} w_\ell^{(2)} = & \frac{1}{\Lambda_f^2} \frac{\theta_{\text{FN}}^2}{\Lambda_f^2} e^c H_d \left[x_e^T (\varphi_T^2 \ell) + x_e^\eta (\eta^2 \ell) + x_e^{\xi''} \xi'' (\varphi_T \ell)' \right] + \\ & + \frac{1}{\Lambda_f^2} \frac{\theta_{\text{FN}}}{\Lambda_f} \mu^c H_d \left[x_\mu^T (\varphi_T^2 \ell)' + x_\mu^\eta (\eta^2 \ell)' + x_\mu^{\xi''} \xi'' (\varphi_T \ell)'' \right] + \\ & + \frac{1}{\Lambda_f^2} \tau^c H_d \left[x_\tau^T (\varphi_T^2 \ell)'' + x_\tau^\eta (\eta^2 \ell)'' + x_\tau^{\xi''} \xi'' (\varphi_T \ell) \right] . \end{aligned} \quad (3.27)$$

To generate both the Yukawa interactions and the soft mass contributions of the RL type, we promote the quantities x_f and $x_f^{T,\eta,\xi''}$ to constant superfields, of the type

$$x_f = y_f - z_f \theta^2 m_0 , \quad x_f^{T,\eta,\xi''} = y_f^{T,\eta,\xi''} - z_f^{T,\eta,\xi''} \theta^2 m_0 \quad (f = e, \mu, \tau) , \quad (3.28)$$

where the coefficients y_f , z_f , $y_f^{T,\eta,\xi''}$ and $z_f^{T,\eta,\xi''}$ are complex numbers of order one. From eqs. (3.26) and (3.27), after the flavour and the electroweak symmetry breakings, the following mass matrix for the charged leptons are obtained:

$$M_\ell = \begin{pmatrix} y_e t^2 u + y_e' t^2 u^2 & c_{T3} y_e t^2 u^2 & c_{T2} y_e t^3 u^2 \\ c_{T2} y_\mu t^2 u^2 & y_\mu t u + y_\mu' t u^2 & c_{T3} y_\mu t u^2 \\ c_{T3} y_\tau u^2 & c_{T2} y_\tau t u^2 & y_\tau u + y_\tau' u^2 \end{pmatrix} \frac{v \cos \beta}{\sqrt{2}} . \quad (3.29)$$

with $y_f' \equiv y_f^T + c^2 y_f^\eta + c_{T1} y_f$. The matrix M_ℓ is shown in the basis in which the kinetic terms are non-canonical. Notice that M_ℓ slightly differs from the corresponding matrix derived in ref. [60] due to the different NLO φ_T vev structure between the AF and the T' models.

Similarly, the neutrino superpotential can be expanded in powers of u :

$$w_\nu = w_\nu^{(1)} + w_\nu^{(2)} + \dots \quad (3.30)$$

The LO term is given by:

$$w_\nu^{(1)} = \frac{x_a}{\Lambda_f \Lambda_L} \xi (H_u \ell H_u \ell) + \frac{x_b}{\Lambda_f \Lambda_L} (\varphi_S H_u \ell H_u \ell) , \quad (3.31)$$

with Λ_L referring to the lepton number violation scale. Also in this case the constants $x_{a,b}$ are promoted to superfields of the form:

$$x_{a,b} = y_{a,b} + z_{a,b} \theta^2 m_0 . \quad (3.32)$$

From this expression for $w_\nu^{(1)}$ one can recover the neutrino mass matrix m_ν of eq. (2.5) simply setting $a = y_a c_a$ and $b = y_b c_b$. The NLO term in the expansion, $w_\nu^{(2)}$, gives rise to order u deviations from the TB mixing scheme. Being not relevant for the subsequent discussion its analytical form will be left out.

The LO and NLO superpotential terms in the u expansion, responsible for the quark masses,

$$w_q = w_q^{(1)} + w_q^{(2)} + \dots \quad (3.33)$$

are respectively given by

$$\begin{aligned} w_q^{(1)} = & x_t (t^c q_3) H_u + \frac{x_b}{\Lambda_f} \theta_{\text{FN}} (b^c q_3) H_d + \\ & + \frac{x_1}{\Lambda_f^2} \theta_{\text{FN}} (\varphi_T D_u^c D_q) H_u + \frac{x_5}{\Lambda_f^2} \theta_{\text{FN}} (\varphi_T D_d^c D_q) H_d + \\ & + \frac{x_2}{\Lambda_f^2} \theta_{\text{FN}} \xi'' (D_u^c D_q)' H_u + \frac{x_6}{\Lambda_f^2} \theta_{\text{FN}} \xi'' (D_d^c D_q)' H_d + \\ & + \frac{1}{\Lambda_f} \left[x_3 t^c (\eta D_q) + \frac{x_4}{\Lambda_f} \theta_{\text{FN}} (D_u^c \eta) q_3 \right] H_u + \\ & + \frac{1}{\Lambda_f^2} \theta_{\text{FN}} \left[x_7 b^c (\eta D_q) + x_8 (D_d^c \eta) q_3 \right] H_d, \end{aligned} \quad (3.34)$$

$$\begin{aligned} w_q^{(2)} = & \frac{x_9}{\Lambda_f^4} \theta_{\text{FN}} \xi^2 (\varphi_S D_u^c D_q) H_u + \frac{x_{11}}{\Lambda_f^4} \theta_{\text{FN}} \xi^2 (\varphi_S D_d^c D_q) H_d + \\ & + \frac{x_{10}}{\Lambda_f^4} \theta_{\text{FN}} (\varphi_S^3 D_u^c D_q) H_u + \frac{x_{12}}{\Lambda_f^4} \theta_{\text{FN}} (\varphi_S^3 D_d^c D_q) H_d + \dots \end{aligned} \quad (3.35)$$

Here dots stand terms which do not introduce new flavour structures in the mass matrices and therefore can be re-absorbed in the parametrisation, as discussed in ref. [1]. The quantities x_i are taken to be constant superfields with

$$x_f = y_f - z_f \theta^2 m_0. \quad (3.36)$$

The up and down quark mass matrices obtained from eqs. (3.34) and (3.35), after the breaking of the flavour and the electroweak symmetries, are given by:

$$\begin{aligned} M_u = & \begin{pmatrix} ic_{T2} y_1 t^2 u^2 + ic_b (c_a^2 y_9 + c_b^2 y_{10}) t u^3 & \left(\frac{1-i}{2}\right) c_{T3} y_1 + c'' y_2 & tu^2 & -c_{\eta_2} y_4 t u^2 \\ \left(\frac{1-i}{2}\right) c_{T3} y_1 - c'' y_2 & tu^2 & y_1 t u & c' y_4 t u \\ c_{\eta_2} y_3 u^2 & & c' y_3 u & y_t \end{pmatrix} \frac{v \sin \beta}{\sqrt{2}}, \\ M_d = & \begin{pmatrix} ic_{T2} y_5 t^2 u^2 + ic_b (c_a^2 y_{11} + c_b^2 y_{12}) t u^3 & \left(\frac{1-i}{2}\right) c_{T3} y_5 + c'' y_6 & tu^2 & -c_{\eta_2} y_8 t u^2 \\ \left(\frac{1-i}{2}\right) c_{T3} y_5 - c'' y_6 & tu^2 & y_5 t u & c' y_8 t u \\ -c_{\eta_2} y_7 t u^2 & & c' y_7 t u & y_b t \end{pmatrix} \frac{v \cos \beta}{\sqrt{2}}. \end{aligned} \quad (3.37)$$

where all the y_i are complex number with absolute value of order one, apart for y_6 which is taken to be slightly larger than its natural value,

$$y_6 \equiv \tilde{y}_6 \frac{1}{\sqrt{t}}, \quad (3.38)$$

in order to reproduce the correct value of the Cabibbo angle (see ref. [1] for more details). Notice that the matrices $M_{u,d}$ are shown in the basis in which the kinetic terms are non-canonical.

The term w_d is responsible for the vacuum alignment of the flavon fields and, at leading and renormalisable order, is given by

$$\begin{aligned}
 w_d = & M (\varphi_T^0 \varphi_T) + g (\varphi_T^0 \varphi_T \varphi_T) + g_7 \xi'' (\varphi_T^0 \varphi_T)' + g_8 (\varphi_T^0 \eta \eta) + \\
 & + g_1 (\varphi_S^0 \varphi_S \varphi_S) + g_2 \tilde{\xi} (\varphi_S^0 \varphi_S) + \\
 & + g_3 \xi^0 (\varphi_S \varphi_S) + g_4 \xi^0 \xi^2 + g_5 \xi^0 \xi \tilde{\xi} + g_6 \xi^0 \tilde{\xi}^2 + \\
 & + M_\eta (\eta^0 \eta) + g_9 (\varphi_T \eta^0 \eta) + \\
 & + M_\xi \xi'^0 \xi'' + g_{10} \xi'^0 (\varphi_T \varphi_T)'' + \dots
 \end{aligned} \tag{3.39}$$

where dots denote sub-leading non-renormalizable corrections. In ref. [1] it has been shown how this superpotential produces the alignment of the flavon vevs. reported in eq. (2.2).

The Froggat-Nielsen flavon θ_{FN} gets its vev through a D -term, once we assume that the symmetry $U(1)_{\text{FN}}$ is gauged. The corresponding scalar potential is:

$$V_{D,\text{FN}} = \frac{1}{2} (M_{\text{FI}}^2 - g_{\text{FN}} |\theta_{\text{FN}}|^2 + \dots)^2 \tag{3.40}$$

where g_{FN} is the gauge coupling constant of $U(1)_{\text{FN}}$ and M_{FI}^2 denotes the contribution of the Fayet-Iliopoulos (FI) term. Dots represent other terms which are not relevant for the calculation of the FN field vev. In the SUSY limit one gets

$$|\langle \theta_{\text{FN}} \rangle|^2 = \frac{M_{\text{FI}}^2}{g_{\text{FN}}} \tag{3.41}$$

which defines the T' symmetry breaking parameter t via eq. (2.2).

Finally the term w_h is associated with the μ parameter:

$$w_h = \mu H_u H_d. \tag{3.42}$$

This term explicitly breaks the continuous $U(1)_R$ symmetry of the model, while preserving the usual R -parity. Furthermore, the soft SUSY breaking term $B\mu$ can then arise from the μ term once μ is promoted to a superfield $\mu + \theta^2 B\mu$.

3.3 Sfermion masses

With the aid of the Kähler potential and of the superpotential written in the previous subsections one can derive the sfermion mass matrices for the T' model. The matter Lagrangian reads:

$$\begin{aligned}
 -\mathcal{L}_m \supset & (\bar{e} \quad \bar{e}^c) \mathcal{M}_e^2 \begin{pmatrix} \tilde{e} \\ \bar{\tilde{e}}^c \end{pmatrix} + \bar{\nu} m_{\nu LL}^2 \tilde{\nu} + \\
 & + (\bar{u} \quad \bar{u}^c) \mathcal{M}_u^2 \begin{pmatrix} \tilde{u} \\ \bar{\tilde{u}}^c \end{pmatrix} + (\bar{d} \quad \bar{d}^c) \mathcal{M}_d^2 \begin{pmatrix} \tilde{d} \\ \bar{\tilde{d}}^c \end{pmatrix},
 \end{aligned} \tag{3.43}$$

where

$$\mathcal{M}_f^2 = \begin{pmatrix} m_{fLL}^2 & m_{fLR}^2 \\ m_{fRL}^2 & m_{fRR}^2 \end{pmatrix}, \quad f = e, u, d. \tag{3.44}$$

with $m_{(f,\nu)LL}^2$ and m_{fRR}^2 being 3×3 hermitian matrices, while $m_{fLR}^2 = (m_{fRL}^2)^\dagger$. Each of these blocks receives contributions from different part of the SUSY Lagrangian:

$$\begin{aligned} m_{(f,\nu)LL}^2 &= (m_{(f,\nu)LL}^2)_K + (m_{(f,\nu)LL}^2)_F + (m_{(f,\nu)LL}^2)_D, \\ m_{fRR}^2 &= (m_{fRR}^2)_K + (m_{fRR}^2)_F + (m_{fRR}^2)_D + (m_{fRR}^2)_{D, \text{FN}}, \\ m_{fRL}^2 &= (m_{fRL}^2)_1 + (m_{fRL}^2)_2 + (m_{fRL}^2)_3. \end{aligned} \quad (3.45)$$

that are going to be described more in details in the following. Notice that in the sneutrino sector only the LL block is present and that any contribution to the sneutrino masses associated to w_ν has been neglected.

The contributions to the sfermion masses from the SUSY breaking terms in the Kähler potential are given by two distinct sources: the first one originates from eqs. (3.3)–(3.13) and is proportional to the parameters s_I . These contributions for the sleptons are given by

$$(m_{(e,\nu)LL}^2)_K = \begin{pmatrix} n_0^\ell + 2n_1^\ell u & n_4^\ell u^2 & n_5^\ell u^2 \\ \bar{n}_4^\ell u^2 & n_0^\ell - (n_1^\ell + n_2^\ell) u & n_6^\ell u^2 \\ \bar{n}_5^\ell u^2 & \bar{n}_6^\ell u^2 & n_0^\ell - (n_1^\ell - n_2^\ell) u \end{pmatrix} m_0^2, \quad (3.46)$$

$$(m_{eRR}^2)_K = \begin{pmatrix} n_1^e & n_4^e u^2 t & n_5^e u^2 t^2 \\ \bar{n}_4^e u^2 t & n_2^e & n_6^e u^2 t \\ \bar{n}_5^e u^2 t^2 & \bar{n}_6^e u^2 t & n_3^e \end{pmatrix} m_0^2, \quad (3.47)$$

while for the squarks are

$$(m_{uLL}^2)_K = (m_{dLL}^2)_K = \begin{pmatrix} n_0^q - n_2^q u & n_5^q u^2 & n_6^q u^2 \\ \bar{n}_5^q u^2 & n_0^q + n_2^q u & n_4^q u \\ \bar{n}_6^q u^2 & \bar{n}_4^q u & n_1^q + n_3^q t^2 \end{pmatrix} m_0^2, \quad (3.48)$$

$$(m_{uRR}^2)_K = \begin{pmatrix} n_0^u - n_2^u u & n_5^u u^2 & n_6^u u^2 t \\ \bar{n}_5^u u^2 & n_0^u + n_2^u u & n_4^u u t \\ \bar{n}_6^u u^2 t & \bar{n}_4^u u t & n_1^u + n_3^u t^2 \end{pmatrix} m_0^2, \quad (3.49)$$

$$(m_{dRR}^2)_K = \begin{pmatrix} n_0^d - n_2^d u & n_5^d u^2 & n_6^d u^2 \\ \bar{n}_5^d u^2 & n_0^d + n_2^d u & n_4^d u \\ \bar{n}_6^d u^2 & \bar{n}_4^d u & n_1^d + n_3^d t^2 \end{pmatrix} m_0^2. \quad (3.50)$$

The coefficients n_i are linearly related to the parameters s_I introduced in eq. (3.16). As such relations do not give any deeper insight, for the rest of the paper n_i will be considered free input parameters, with absolute values of order one. All these coefficients are in general complex, with the obvious exception of the ones appearing in the diagonal, that, for hermiticity, are real. In addition, one assumes n_0^ℓ , $n_{1,2,3}^e$ and $n_{0,1}^{q,u,d}$ positive, in order to have positive definite squared masses, to avoid electric-charge breaking minima and further sources of electroweak symmetry breaking.

The second contribution to sfermion masses coming from the Kähler potential is related to the auxiliary fields of the flavon supermultiplets, that acquire non-vanishing vevs, as

shown in eq. (2.10), when soft SUSY breaking terms are included into the flavon potential. This type of contribution originates from a fourth derivative term of the Kähler potential:

$$\left\langle \frac{\partial^4 \mathcal{K}}{\partial f_i \partial \bar{f}_j \partial \Phi_k \partial \bar{\Phi}_l} \right\rangle \left\langle \frac{\partial w}{\partial \Phi_k} \right\rangle \overline{\left\langle \frac{\partial w}{\partial \Phi_l} \right\rangle} \tilde{f}_i \tilde{f}_j, \quad (3.51)$$

where f refers to the matter scalar fields and Φ to the flavons. For completeness all these contributions are explicitly derived in appendix B, where it is also shown how these terms can be safely absorbed in a redefinition of the coefficients n_i .

The SUSY contribution from the F terms is completely negligible for sneutrinos, while for charged sfermions they read:

$$\begin{aligned} (m_{eLL}^2)_F &= M_\ell^\dagger [(K^e)^{-1}]^T M_\ell, & (m_{eRR}^2)_F &= M_\ell (K^\ell)^{-1} M_\ell^\dagger, \\ (m_{uLL}^2)_F &= M_u^\dagger [(K^u)^{-1}]^T M_u, & (m_{uRR}^2)_F &= M_u (K^q)^{-1} M_u^\dagger, \\ (m_{dLL}^2)_F &= M_d^\dagger [(K^d)^{-1}]^T M_d, & (m_{dRR}^2)_F &= M_d (K^q)^{-1} M_d^\dagger, \end{aligned} \quad (3.52)$$

where M_f is the fermion mass matrix and K^f is the matrix specifying the kinetic terms, explicitly written in eqs. (3.19)–(3.23).

The SUSY contribution from the D terms are given by:

$$\begin{aligned} (m_{eLL}^2)_D &= \left(-\frac{1}{2} + \sin^2 \theta_W \right) \cos 2\beta m_Z^2 K^\ell, \\ (m_{eRR}^2)_D &= (-1) \sin^2 \theta_W \cos 2\beta m_Z^2 (K^e)^T, \\ (m_{\nu LL}^2)_D &= \left(+\frac{1}{2} \right) \cos 2\beta m_Z^2 K^\ell, \\ (m_{uLL}^2)_D &= \left(+\frac{1}{2} - \frac{2}{3} \sin^2 \theta_W \right) \cos 2\beta m_Z^2 K^q, \\ (m_{uRR}^2)_D &= \left(+\frac{2}{3} \right) \sin^2 \theta_W \cos 2\beta m_Z^2 (K^u)^T, \\ (m_{dLL}^2)_D &= \left(-\frac{1}{2} + \frac{1}{3} \sin^2 \theta_W \right) \cos 2\beta m_Z^2 K^q, \\ (m_{dRR}^2)_D &= \left(-\frac{1}{3} \right) \sin^2 \theta_W \cos 2\beta m_Z^2 (K^d)^T, \end{aligned} \quad (3.53)$$

where m_Z is the Z mass and θ_W is the Weinberg angle. For all the right-handed fields but t^c an additional D term contribution, coming from the gauged $U(1)_{FN}$ sector, is present. One can check that this contribution can be simply reabsorbed in the redefinition of the $n_i^{e,u,d}$ coefficients parametrizing $(m_{fRR}^2)_K$.

Concerning the RL mass blocks, they are the results of three distinct terms: the first one originates from the superpotential, eqs. (3.26), (3.27), (3.34), (3.35), and is proportional to the parameters z_f and z'_f of the decomposition in eqs. (3.28), (3.36):

$$(m_{(e,d)RL}^2)_1 = A_1^{(e,d)} \frac{v \cos \beta}{\sqrt{2}} A_0, \quad (m_{uRL}^2)_1 = A_1^u \frac{v \sin \beta}{\sqrt{2}} A_0, \quad (3.54)$$

with A_0 a common (SUSY) trilinear mass term and where for the sleptons we have defined

$$A_1^e = \begin{pmatrix} z_e t^2 u + z'_e t^2 u^2 & c_{T3} z_e t^2 u^2 & c_{T2} z_e t^3 u^2 \\ c_{T2} z_\mu t^2 u^2 & z_\mu t u + z'_\mu t u^2 & c_{T3} z_\mu t u^2 \\ c_{T3} z_\tau u^2 & c_{T2} z_\tau t u^2 & z_\tau u + z'_\tau u^2 \end{pmatrix}, \quad (3.55)$$

with $z'_i = z_f^T + c'^2 z_i^\eta + c_{T1} z_i$ for $i = e, \mu, \tau$, while for the squarks we have

$$A_1^u = \begin{pmatrix} i c_{T2} z_1 t^2 u^2 + i z_9 t u^3 & \left(\frac{1-i}{2} c_{T3} z_1 + c'' z_2\right) t u^2 - c_{\eta_2} z_4 t u^2 \\ \left(\frac{1-i}{2} c_{T3} z_1 - c'' z_2\right) t u^2 & z_1 t u & c' z_4 t u \\ -c_{\eta_2} z_3 u^2 & c' z_3 u & z_t \end{pmatrix}, \quad (3.56)$$

$$A_1^d = \begin{pmatrix} i c_{T2} z_5 t^2 u^2 + i z_{11} t u^3 & \left(\frac{1-i}{2} c_{T3} z_5 + c'' z_6\right) t u^2 - c_{\eta_2} z_8 t u^2 \\ \left(\frac{1-i}{2} c_{T3} z_5 - c'' z_6\right) t u^2 & z_5 t u & c' z_8 t u \\ -c_{\eta_2} z_7 t u^2 & c' z_7 t u & z_b t \end{pmatrix}, \quad (3.57)$$

with $z_9 = c_b(c_a^2 z_9 + c_b^2 z_{10})$ and $z_{11} = c_b(c_a^2 z_{11} + c_b^2 z_{12})$. Notice that the matrix A_1^e in eq. (3.55) differs from the corresponding matrix in ref. [60], the reason being the, already mentioned, different choice of the flavon φ_T vev.

The second term in the LR mass matrices has the same source of eq. (3.51) and it is related to the non-vanishing vev of the auxiliary fields of the flavon supermultiplets. This contribution can be written as

$$\left\langle \frac{\partial^3 w}{\partial \Phi \partial f_i^c \partial f_j} \right\rangle \overline{\left\langle \frac{\partial w}{\partial \Phi} \right\rangle} \tilde{f}_i^c \tilde{f}_j + \text{h.c.} \quad (3.58)$$

so that the soft mass matrices $(m_{fRL}^2)_2$ read as

$$(m_{(e,d)RL}^2)_2 = A_2^{(e,d)} \frac{v \cos \beta}{\sqrt{2}} A_0, \quad (m_{uRL}^2)_2 = A_2^u \frac{v \sin \beta}{\sqrt{2}} A_0. \quad (3.59)$$

The matrices $A_2^{(e,u,d)}$ have exactly the same structure of $A_1^{(e,u,d)}$ in eqs. (3.55)–(3.57) in terms of u and t , apart from the (3,3) entries of $A_2^{(u,d)}$ which are vanishing. Furthermore only the coefficients of order one are different. As it will be discussed in the next section, these two contributions cannot be absorbed into the same matrix, by a simple redefinition of the parameters. When moving to the physical basis, in the $A_1^{(e,u,d)}$ matrices several cancellations among the parameters happen, while this is not the case for the $A_2^{(e,u,d)}$ matrices. Consequently, these two contributions are kept distinct and the explicit form of $A_2^{(e,u,d)}$ follows from that of $A_1^{(e,u,d)}$ in eqs. (3.55)–(3.57), simply substituting $\{z_f, z'_f, z_i, c_i\}$ with $\{\bar{c}^F y_f, y_f^F, y_i, \bar{c}_i^F\}$, where $f = e, \mu, \tau$ and $i = 1, \dots, 11$. The new parameters in this list are

$$\begin{aligned} y_f^F &= 2\bar{c}^F y_f^T + 2\bar{c}^{F'} y_f^\eta + \bar{c}_{T1}^F y_f, \\ y_9^F &= 2c_a(\bar{c}_a^F c_b + c_a \bar{c}_b^F) y_9 + 3\bar{c}_b^F c_b^2 y_{10}, \\ y_{11}^F &= 2c_a(\bar{c}_a^F c_b + c_a \bar{c}_b^F) y_{11} + 3\bar{c}_b^F c_b^2 y_{12}. \end{aligned} \quad (3.60)$$

Finally, the last contribution to the LR mass matrices is proportional to the fermion masses and explicitly depends on $\tan\beta$ through:

$$(m_{(e,d)RL}^2)_3 = -\bar{\mu} \tan\beta M_{(\ell,d)}, \quad (m_{uRL}^2)_3 = -\bar{\mu} \frac{1}{\tan\beta} M_u. \quad (3.61)$$

The origin of this contribution is quite similar to the previous one, since it also arises from the auxiliary component of a superfield: the terms in eq. (3.59) originate from the auxiliary component of the flavon superfields, while the terms in eq. (3.61) from the auxiliary component associated to the Higgs doublets H_d and H_u .

4 The physical basis

All the matrices of the previous section are written in a basis in which the kinetic terms of (s)fermion are non-canonical. To have a better phenomenological insight, it is useful to move to a *physical* basis defined as a basis in which the kinetic terms are in a canonical form and the charged lepton and down quark matrices are diagonal. All matrices in the *physical* basis are going to be denoted with a hat. Most of the details of this basis change are deferred to the appendices B and C.

In the preferred allowed T' -breaking parameters space one has that $u \approx t \approx \lambda^2$. In terms of powers of the flavour symmetry breaking parameters u and t , the charged fermion mass matrices in the *physical* basis read

$$\hat{M}_\ell \sim \text{diag}(t^2 u, t u, u), \quad \hat{M}_d \sim \text{diag}(u^3, t u, t), \quad \hat{M}_u \sim \begin{pmatrix} \sqrt{t} u^3 & t u^2 & t u^2 \\ \sqrt{t} u^2 & t u & t u \\ \sqrt{t} u & u & 1 \end{pmatrix}. \quad (4.1)$$

As exemplification we can show here how it is possible to recover the correct V_{CKM} structure and to obtain the experimental values just selecting appropriate order one value for the model unknown coefficients entering in the mixing matrix. The derivation follows straightforwardly from ref. [1], inserting explicitly the substitution in eq. (3.38) and the vev alignment for φ_T in eq. (2.2). From eqs. (51) of ref. [1] one obtains the following identification between the CKM parameters in the Wolfenstein parametrisation and the T' model coefficients:

$$\lambda = -\frac{\tilde{y}_6}{y_5} c'' \frac{u}{\sqrt{t}}, \quad A = \left(\frac{y_7}{y_b} - \frac{y_3}{y_t} \right) \frac{\tilde{y}_6^2}{y_5^2} \frac{c' t}{c'' u}. \quad (4.2)$$

These expressions automatically lead to a consistent identification of the leading 13 and 31 CKM elements,

$$V_{td} \sim V_{ub} \approx A \lambda^3 = \left(\frac{y_7}{y_b} - \frac{y_3}{y_t} \right) \frac{\tilde{y}_6}{y_5} c' c'' \frac{u^2}{\sqrt{t}}, \quad (4.3)$$

while leave enough freedom for recovering the experimental (order one) values for the last two CKM parameters ρ and η . The corresponding expressions in terms of the T' order one coefficients can be easily derived but are not reported here not particularly suggestive.

Moving to the physical basis and performing the corresponding transformations to the sfermion sector give quite involved results. Here only the naive structure of the sfermion mass matrices in terms of the T' breaking parameters u and t are showed, thus omitting all the order one unknown coefficients of the model. A complete description can be found in appendix B. Starting with the LL block, the Kähler potential contributions are given by

$$(\hat{m}_{(e,\nu)LL}^2)_K \sim \begin{pmatrix} 1+u & u^2 & u^2 \\ u^2 & 1+u & u^2 \\ u^2 & u^2 & 1+u \end{pmatrix} m_0^2 \quad (4.4)$$

for the sleptons and

$$(\hat{m}_{(u,d)LL}^2)_K \sim \begin{pmatrix} 1+u & u\sqrt{t} & u\sqrt{t} \\ u\sqrt{t} & 1+u & u \\ u\sqrt{t} & u & 1 \end{pmatrix} m_0^2 \quad (4.5)$$

for the squarks.

The supersymmetric F and D term contributions are respectively given by

$$\begin{aligned} (\hat{m}_{eLL}^2)_F &= \hat{M}_\ell^T \hat{M}_\ell, & (\hat{m}_{\nu LL}^2)_F &= 0, \\ (\hat{m}_{uLL}^2)_F &= \hat{M}_u^T \hat{M}_u, & (\hat{m}_{dLL}^2)_F &= \hat{M}_d^T \hat{M}_d, \end{aligned} \quad (4.6)$$

and by

$$(m_{eLL}^2)_D = \left(-\frac{1}{2} + \sin^2 \theta_W \right) \cos 2\beta m_Z^2 \times \mathbb{1}, \quad (4.7)$$

$$(m_{\nu LL}^2)_D = \left(+\frac{1}{2} \right) \cos 2\beta m_Z^2 \times \mathbb{1}, \quad (4.8)$$

$$(m_{uLL}^2)_D = \left(+\frac{1}{2} - \frac{2}{3} \sin^2 \theta_W \right) \cos 2\beta m_Z^2 \times \mathbb{1}, \quad (4.9)$$

$$(m_{dLL}^2)_D = \left(-\frac{1}{2} + \frac{1}{3} \sin^2 \theta_W \right) \cos 2\beta m_Z^2 \times \mathbb{1}. \quad (4.10)$$

Both, F and D term contributions are suppressed by a factor of order $\hat{M}_f^T \hat{M}_f / m_0^2$ or order m_Z^2 / m_0^2 , respectively, compared to those coming from the Kähler potential and so numerically negligible for typical values of m_0 around 1 TeV.

The Kähler potential contributions to the RR block of the slepton, up- and down-squark matrices are respectively

$$(\hat{m}_{eRR}^2)_K \sim \begin{pmatrix} 1 & \frac{m_e}{m_\mu} u & \frac{m_e}{m_\tau} u \\ \frac{m_e}{m_\mu} u & 1 & \frac{m_\mu}{m_\tau} u \\ \frac{m_e}{m_\tau} u & \frac{m_\mu}{m_\tau} u & 1 \end{pmatrix} m_0^2, \quad (4.11)$$

$$(\hat{m}_{uRR}^2)_K \sim \begin{pmatrix} 1+u & u^2 & t u^2 \\ u^2 & 1+u & t u \\ t u^2 & t u & 1 \end{pmatrix} m_0^2, \quad (4.12)$$

$$(\hat{m}_{dRR}^2)_K \sim \begin{pmatrix} 1+u & u \sqrt{t} & u \sqrt{t} \\ u \sqrt{t} & 1+u & u \\ u \sqrt{t} & u & 1 \end{pmatrix} m_0^2. \quad (4.13)$$

The supersymmetric F and D contributions read:

$$\begin{aligned} (\hat{m}_{eRR}^2)_F &= \hat{M}_\ell \hat{M}_\ell^T, \\ (\hat{m}_{uRR}^2)_F &= \hat{M}_u \hat{M}_u^T, \quad (\hat{m}_{dRR}^2)_F = \hat{M}_d \hat{M}_d^T, \end{aligned} \quad (4.14)$$

and

$$\begin{aligned} (m_{eRR}^2)_D &= (-1) \sin^2 \theta_W \cos 2\beta m_Z^2 \times \mathbb{1}, \\ (m_{uRR}^2)_D &= \left(+\frac{2}{3}\right) \sin^2 \theta_W \cos 2\beta m_Z^2 \times \mathbb{1}, \\ (m_{dRR}^2)_D &= \left(-\frac{1}{3}\right) \sin^2 \theta_W \cos 2\beta m_Z^2 \times \mathbb{1}. \end{aligned} \quad (4.15)$$

Also in this case the SUSY contributions are numerically negligible in most of the parameter space.

Finally, the contributions to the RL block for charged sfermions read

$$(\hat{m}_{eRL}^2)_1 \sim \begin{pmatrix} m_e & m_e u & m_e u \\ m_\mu t u^2 & m_\mu & m_\mu u \\ m_\tau u^2 & m_\tau t u^2 & m_\tau \end{pmatrix} A_0. \quad (4.16)$$

$$(\hat{m}_{eRL}^2)_2 \sim \begin{pmatrix} m_e & m_e u & m_e u \\ m_\mu u & m_\mu & m_\mu u \\ m_\tau u & m_\tau u & m_\tau \end{pmatrix} A_0, \quad (4.17)$$

$$(\hat{m}_{eRL}^2)_3 = -\mu^\dagger \tan \beta \hat{M}_\ell. \quad (4.18)$$

An important feature of $(\hat{m}_{eRL}^2)_1$ is that the elements below the diagonal are suppressed by a factor $\sim u$ compared to the corresponding elements of the matrix in the non-canonical

basis. However, this fact does not happen for $(\hat{m}_{eRL}^2)_2$. As a result the elements of $(\hat{m}_{eRL}^2)_2$ dominate with respect to those of $(\hat{m}_{eRL}^2)_1$.

The RL matrix for the up squarks sector is given by the three following contributions:

$$(\hat{m}_{uRL}^2)_1 \sim \begin{pmatrix} \sqrt{t}u^3 & tu^2 & tu \\ \sqrt{t}u^2 & tu & u \\ u^2/\sqrt{t} & u & 1 \end{pmatrix} \frac{v \sin \beta}{\sqrt{2}} A_0, \quad (4.19)$$

$$(\hat{m}_{uRL}^2)_2 \sim \begin{pmatrix} tu^2 & tu^2 & tu^2 \\ \sqrt{t}u^2 & tu & tu \\ u^2/\sqrt{t} & u & u^2 \end{pmatrix} \frac{v \sin \beta}{\sqrt{2}} A_0, \quad (4.20)$$

$$(\hat{m}_{uRL}^2)_3 = -\mu^\dagger \frac{1}{\tan \beta} \hat{M}_u. \quad (4.21)$$

Comparing these results with the un-hatted matrices of eqs. (3.54) and (3.59), one can observe that the first column of $(\hat{m}_{uRL}^2)_1$ is enhanced by a factor $t^{-1/2}$, while the entry (13) of $(\hat{m}_{uRL}^2)_1$ is enhanced by a factor u^{-1} . Also the first column of $(\hat{m}_{uRL}^2)_2$ is increased by a factor $t^{-1/2}$ with respect to $(m_{uRL}^2)_2$, except for the (11) entry which is, instead, enhanced by a factor t^{-1} . Moreover the entry (33) of $(\hat{m}_{uRL}^2)_2$ is not vanishing as in $(m_{uRL}^2)_2$, but it is proportional to u^2 .

Finally the down squarks LR contributions are the following:

$$(\hat{m}_{dRL}^2)_1 \sim \begin{pmatrix} u^3 & \sqrt{t}u^2 & \sqrt{t}u^2 \\ \sqrt{t}u^2 & tu & tu \\ \sqrt{t}u^2 & tu & t \end{pmatrix} \frac{v \cos \beta}{\sqrt{2}} A_0, \quad (4.22)$$

$$(\hat{m}_{dRL}^2)_2 \sim \begin{pmatrix} u^3 & \sqrt{t}u^2 & \sqrt{t}u^2 \\ \sqrt{t}u^2 & tu & tu \\ \sqrt{t}u^2 & tu & tu^2 \end{pmatrix} \frac{v \cos \beta}{\sqrt{2}} A_0, \quad (4.23)$$

$$(\hat{m}_{dRL}^2)_3 = -\mu^\dagger \tan \beta \hat{M}_d. \quad (4.24)$$

The first column of $(\hat{m}_{dRL}^2)_{1,2}$ shows the same enhancement, compared to the un-hatted matrices of eqs. (3.54) and (3.59), as for the up-type squarks, while the entry (33) of $(\hat{m}_{dRL}^2)_2$ is not vanishing as in $(m_{dRL}^2)_2$, but scales as tu^2 .

5 Phenomenology of the T' FCNC sector

While several flavour models can account for the correct SM mass and mixing patterns, a discrimination between them can only be obtained through a detailed analysis of the associated phenomenology. This section will be dedicated to study the predictions of the T' model to the most relevant, leptonic and hadronic, FCNC observables. The results

for the FCNC leptonic sector are going to be a straightforward replica of those obtained in ref. [60] for the A_4 model, as the two realisations (almost) coincide when restricted to leptons: only slight differences are expected from the extra flavons η and ξ'' (see eq. (2.2)) that are included when the embedding of A_4 in T' is considered. No corresponding analysis, instead, has ever been performed on the T' predictions for the FCNC hadronic sector. Therefore the main goal of this section will be twofold: from one side we will explore the T' model constraints coming from the hadronic sector; from the other side, we will combine such constraints with those arising from the leptonic sector. This combined analysis will help in better identifying which cross-correlations can be most useful in discriminating between several (discrete) flavour models.

As discussed in the previous sections both the fermion and sfermion flavour structures are obtained in our model in terms of the two T' symmetry breaking parameters u and t . While t governs essentially the charged fermion mass hierarchy, the amount of flavour changing is proportional to the u parameter. The allowed range in which u and t can be varied is constrained by the experimental data on lepton masses and mixings. As stated in section 2 one gets $t \simeq 0.05$ and $0.007 \lesssim u \lesssim 0.05$. The allowed values of $\tan \beta$ are fixed by the requirement that the τ mass is consistent with experimental data (see eq. (2.4)) giving a range $2 \lesssim \tan \beta \lesssim 15$ for $u = 0.05$ while for $u = 0.007$ only $\tan \beta \simeq 2$ is permitted.

Although it is not possible to set consistently $u = 0$, as viable fermion masses and mixings cannot be obtained, an interesting limit is found when $u = 0$ is selected only in the sfermion sector. Indeed, at the high energy scale $\Lambda_f \approx M_{GUT}$, the SUSY scalar sector very much resembles the MSUGRA framework, with the scalar mass matrices function of the common, flavour universal, soft bilinear and trilinear parameters (m_0, A_0) . This fact is inherited from the underlying assumption that all the SUSY breaking of the model is provided by a unique (hidden) sector. However, our construction deviates from plain MSUGRA due to the different T' embedding of the matter fields that permits, also in the $u = 0$ limit, non-universal (order one) diagonal soft terms in the sfermion mass matrices, as it appears evident, for example, from eqs. (3.3) and (3.11). The flavour symmetry G_f does not predict the parameters involved either in the gaugino or in the Higgs(ino) sectors. Therefore, inspired by MSUGRA, a common gaugino mass $M_{1/2}$ and a common scalar mass m_0 are assumed at the high energy scale Λ_f . The μ parameter is fixed by imposing the requirement of a correct EW symmetry breaking: it can be expressed as a (one-loop) function of the other MSUGRA parameters, with the only freedom of the sign $[\mu]$.

Due to all these constraints, one expects our T' model to (almost) approximate MSUGRA, in the small u region, while significant deviations can be, instead, expected only in the large u (and large $\tan \beta$) region. We will concentrate on the two most compelling cases:

- A) the (almost) universal “limit” $u = 0.01$, with $\tan \beta = 5$. In this scenario one does not expect any sizable difference between the T' and the MSUGRA FCNC phenomenology.³
In the following we will refer to this case as *Reference Point A* (RP_A);

³The lowest allowed value for $(u, \tan \beta)$ is $(0.007, 2)$, for which it turns out to be statistically harder to found a physically allowed SUSY spectrum, due to the smallness of $\tan \beta$. No significant phenomenological difference can be seen with respect to the considered case.

B) the non-universal “limit” $u = 0.05$ with $\tan\beta = 15$. In this scenario one has the strongest allowed deviation from the universal soft breaking term case. The T' model might be experimentally distinguished from the MSUGRA assumption. We will refer to this case as *Reference Point B* (RP_B);

Regarding the scalar bilinear and trilinear parameters we will show the results for two different choices: low ($A_0 = 2m_0 = 400$ GeV) and high ($A_0 = 2m_0 = 2000$ GeV) soft breaking scale, with the gaugino mass term spanning in the $100 < M_{1/2} < 1000$ GeV range.

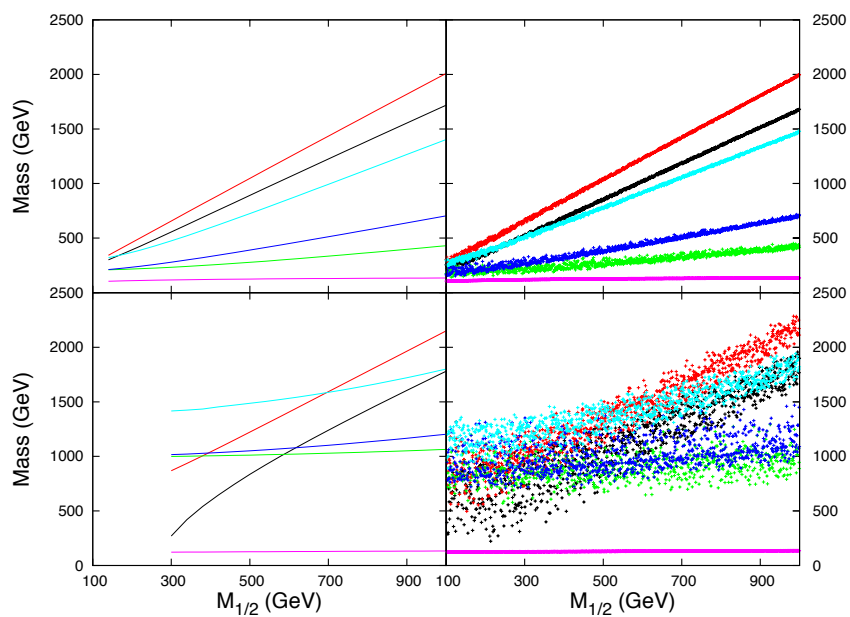
5.1 SUSY mass spectrum: MSUGRA vs. T'

The SUSY spectrum at low energies has been obtained by means of the code `SPheno-2.2.3` [66]. This program implements SUSY one-loop (and partially two loops) Renormalisation Group Equations (RGE) from the high energy scale where the model parameters are defined, down to the electroweak scale, where observables are measured. This procedure is performed in an iterative way until a stable (under RGE) SUSY low energy spectrum is obtained. Even if the default algorithm deals with universal boundary conditions, typical of the MSUGRA setting, it is already built in the possibility to account for non-diagonal Yukawas and soft terms, as in the MSSM.

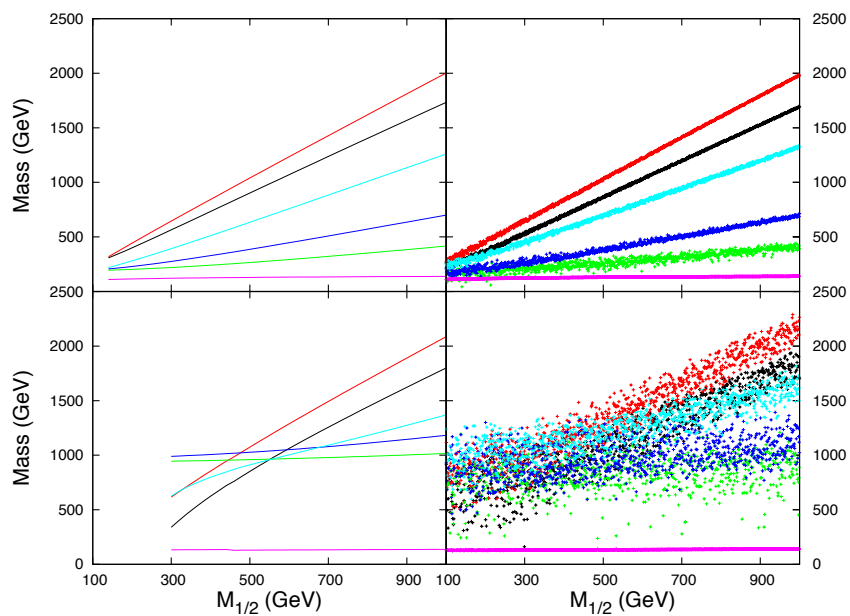
Using this general framework we have implemented in `SPheno` our T' model in a consistent way, i.e. by requiring that the iteration procedure does not spoil the agreement with the physical values of fermionic masses and mixing, also predictions of the model. In practice, the structures of the high energy fermion and sfermion mass matrices introduced in `SPheno` are the ones given in section 4 in the *physical* basis. At the end of the iteration, the stable set of SUSY masses are used for calculating the corrections to the fermionic masses and mixings at the EW scale (see ref. [66]). Consistency at 1σ level with the known SM flavour (low energy) parameters [2] is obtained by accordingly fixing the (order one) values of few of the T' free parameters. All the other T' coefficients are, instead, considered as free order-one parameters, with an absolute value chosen randomly in the $(1/2, 2)$ range.

This procedure is simultaneously “natural” and “stable”. Natural because only order one values for all the T' parameters (let fixed or free) are chosen. Stable because once the fixed T' parameter are set, the effect on the SM parameters of choosing random (order one) free T' parameters is negligible. Notice, moreover, that fixing some of the T' parameters does not introduce any fine-tuning in the model, as it has been exemplified in the previous section for the V_{CKM} case. This procedure in principle can restrict the SUSY spectrum obtained at low energy, as a consequence of the combined RGE evolution. However, this effect is (partially) compensated by the presence of the many free (order one) parameters in the soft SUSY sector.

In figure 1 we compare the MSUGRA scalar spectrum (left plots) with the T' model one (right plots), as function of common gaugino mass $M_{1/2}$. The results in figure 1(a) refer to the RP_A case (i.e. $u = 0.01$ and $\tan\beta = 5$) while the plots in figure 1(b) cover the RP_B case (i.e. $u = 0.05$ and $\tan\beta = 15$). In each figure, the two upper plots are shown for a common bilinear and trilinear scalar SUSY scale $A_0 = 2m_0 = 400$ GeV, while for the two



(a) MSUGRA (left) vs. T' (right) spectra for $u = 0.01$ and $\tan\beta = 5$. In the upper (lower) plots $A_0 = 2m_0 = 400$ GeV ($A_0 = 2m_0 = 2000$ GeV).



(b) MSUGRA (left) vs. T' (right) spectra for $u = 0.05$ and $\tan\beta = 15$. In the upper (lower) plots $A_0 = 2m_0 = 400$ GeV ($A_0 = 2m_0 = 2000$ GeV).

Figure 1. SUSY scalar spectra. The colors in the plots refer respectively to: Magenta for h^0 , Green for $\tilde{\ell}$, Blue for $\tilde{\nu}$, Cyan for H^\pm , Black for \tilde{t} , and Red for \tilde{b} .

lower plots $A_0 = 2m_0 = 2000$ GeV has been chosen. For definiteness only the $\text{sign}[\mu] > 0$ results have been shown, as no significative dependence on it is expected, nor observed.

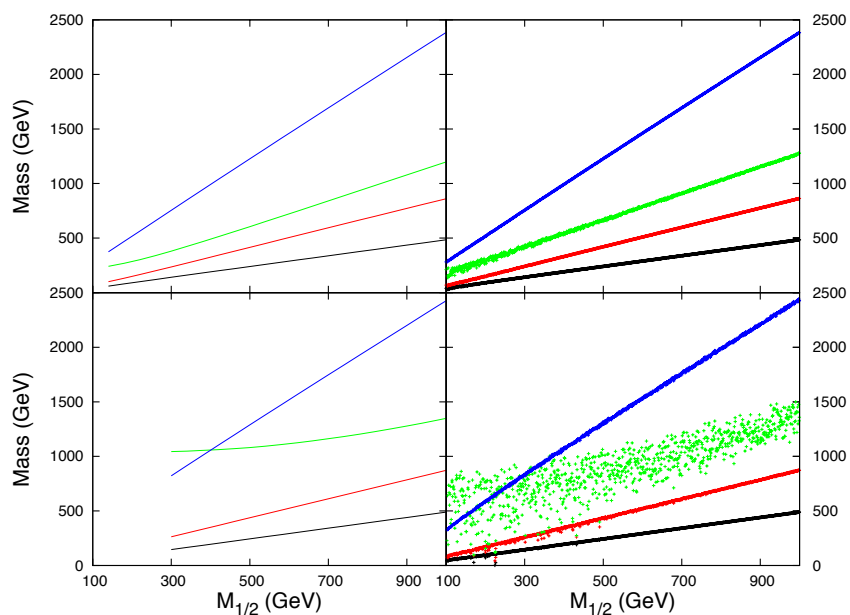
The SM-like Higgs particle (in Magenta) is almost insensitive on the gaugino mass parameter. Only points of the parameter space surviving the LEP2 lower bound are considered. The SUSY lightest scalar is typically the $\tilde{\tau}_1$ (in Green) except for large m_0 and small $M_{1/2}$ where the (right-handed) \tilde{t}_1 is lighter (in Black). In Blue is shown the lightest sneutrino, $\tilde{\nu}_1$, while in Red the lightest sbottom, \tilde{b}_1 . All the other sfermions are not shown in the plot. However all the (almost) left-handed sleptons are practically degenerate with the $\tilde{\nu}_1$, while the (almost) right-handed are degenerate with the $\tilde{\tau}_1$. The first two family squarks are heavier than \tilde{b}_1 and \tilde{t}_1 and nearly degenerate. Finally, the charged Higgs (in Cyan) can be the heaviest particle of the spectrum in the large m_0 and small $M_{1/2}$ region.

As it can be noticed, comparing the left with the right plot of figure 1, the SUSY scalar spectra for MSUGRA and T' are very similar for small m_0 value (upper plots) while two evident differences appear when going to heavier scalar masses (lower plots). The first difference can be noticed in the low $M_{1/2}$ region where the T' spectrum always extends to lower $M_{1/2}$ compared with the MSUGRA one. This happens because of the “phenomenological” requirements that have been imposed on Higgs and SUSY masses⁴ In the T' model, due to the freedom in the choice of the (order one) diagonal and off-diagonal parameters, one can always have a physically allowed spectrum down $M_{1/2} \sim 100$ GeV. The second evident difference is represented by a broadening of all scalar masses, but the lightest Higgs. This effects can be already noticed in the $m_0 = 200$ GeV plot, and then it is strongly enhanced for large values of m_0 and A_0 . The reason of such a broadening is related to the strong dependence that these masses have from the order one (randomly chosen in the $(1/2, 2)$ range) free T' coefficients. Nevertheless, still in this case, the “average” T' scalar masses agree quite well with the MSUGRA predictions.

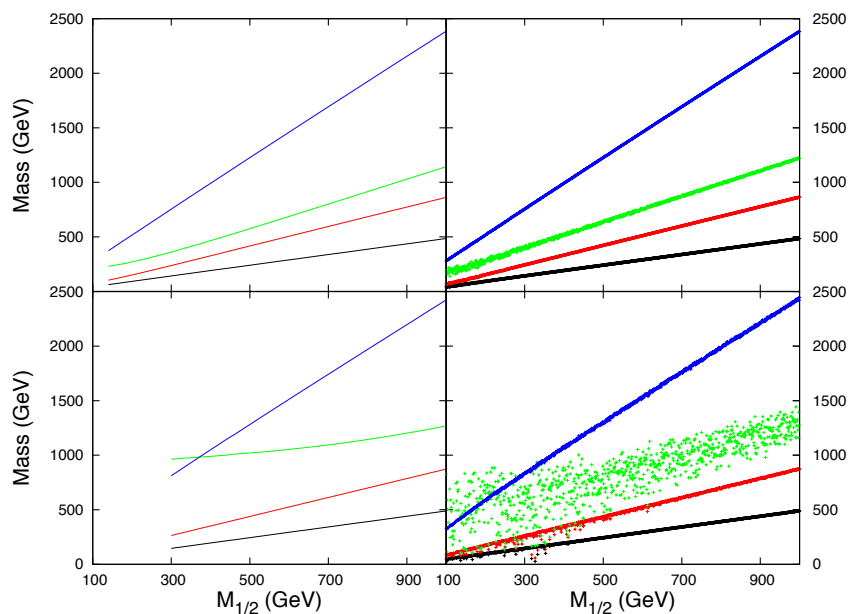
In figure 2 we compare the MSUGRA fermionic spectrum (left plots) with the T' model one (right plots), as function of common gaugino mass $M_{1/2}$. The results in figure 2(a) refer to the RP_A case, while the plots in figure 2(b) cover the RP_B case. In each figure the two upper plots are shown for a common bilinear and trilinear scalar SUSY scale $A_0 = 2m_0 = 400$ GeV, while for the two lower plots $A_0 = 2m_0 = 2000$ GeV has been chosen. For definiteness, again, only the $\text{sign}[\mu] > 0$ results have been shown, as no significative dependence on it is expected, nor observed.

As typical in the MSUGRA framework, the lightest supersymmetric fermion is the lightest neutralino $\tilde{\chi}_1^0$ (in Black), while the lightest chargino $\tilde{\chi}_1^+$ is almost degenerate to the next-to-lightest neutralino $\tilde{\chi}_2^0$ (in Red). The gluino is typically the heaviest fermion (in Blue). As it can be noticed, comparing the upper left with the upper right plots of figures 2(a) and 2(b), the SUSY fermionic spectra for MSURGRA and T' look very similar for small m_0 values, while evident differences appear in the large m_0 case. Again, for $m_0 = 1000$ GeV one can notice that the T' spectrum is “phenomenologically” allowed down to $M_{1/2} \sim 100$ GeV, while the MSUGRA one stops to be acceptable at $M_{1/2} \sim 300$ GeV. The

⁴Specifically, we assumed a Higgs mass $m_H > 114$ GeV, lightest chargino and slepton masses $m_{\tilde{\chi}_1^+}, m_{\tilde{\ell}} > 100$ GeV, as well as the neutralino being the LSP.



(a) MSUGRA (left) vs. T' (right) spectra for $u = 0.01$ and $\tan\beta \approx 5$. In the upper (lower) plots $A_0 = 2m_0 = 400$ GeV ($A_0 = 2m_0 = 2000$ GeV).



(b) MSUGRA (left) vs. T' (right) spectra for $u = 0.05$ and $\tan\beta \approx 15$. In the upper (lower) plots $A_0 = 2m_0 = 400$ GeV ($A_0 = 2m_0 = 2000$ GeV).

Figure 2. SUSY fermion spectra. The colors in the plots refer respectively to: Black for $\tilde{\chi}_1^0$, Red for $\tilde{\chi}_2^0$ and $\tilde{\chi}_1^+$, Green for $\tilde{\chi}_{3,4}^0$ and $\tilde{\chi}_2^+$, and Blue for \tilde{g} .

second evident difference, as in the scalar case, is the presence of the broadening. However, differently from the scalar case, this effect appears only in the mass of next-to-heaviest gauginos (in Green), associated to the (mostly) higgsino-like chargino and neutralino, $\tilde{\chi}_2^+$, $\tilde{\chi}_{3,4}^0$. The reason for such a broadening is due to the way the μ -parameter is derived: while in MSUGRA, $|\mu|$ is uniquely fixed once all the common SUSY parameters are defined, in our model μ indirectly depends also from the randomly chosen (order one) parameters that enter in the sfermion mass matrices. This freedom largely affects the derived value of $|\mu|$ especially in the large (m_0, A_0) region.

5.2 FCNC in the leptonic sector

The LFV analysis of the T' model is going to be a straightforward replica of that performed in ref. [60] for the A_4 realisation, as the two models (almost) coincide when restricted to the leptonic sector. As already stated in the previous sections, only slight differences are expected due to the presence of the extra flavons η and ξ'' (see eq. (2.2)) that are introduced when the embedding of A_4 in T' is considered. The only relevant improvement, compared to the A_4 analysis of ref. [60], is the implementation here of the complete (one-loop) RGE running of the high-energy model parameters down to the EW scale, that leads to a somehow heavier SUSY spectrum when compared to the un-ran case. In order to compare the T' and A_4 predictions, the T' branching ratio for $\mu \rightarrow e\gamma$ is shown in figure 3 as a function of the common gaugino scale $M_{1/2}$. The full horizontal line represents the recently reported 90% C.L. MEG upper limit ref. [67] of 2.4×10^{-12} on the $\text{BR}(\mu \rightarrow e\gamma)$, while the dashed line shows, for comparison, the old MEGA bound of 1.2×10^{-11} .

The two upper plots refer to $A_0 = 2m_0 = 400$ GeV, respectively for the RP_A case (upper-left) and RP_B case (upper-right). Red points are excluded either by the direct experimental requirements on the light Higgs or SUSY masses (mainly in the low $M_{1/2}$ region), or by the requirement of a neutral LSP (mainly in the high $M_{1/2}$ region where the $\tilde{\tau}_1$ becomes lighter than the $\tilde{\chi}_1^0$). Blue (Green) points refer to $\mu > 0$ ($\mu < 0$) respectively. No significative dependence on the $\text{sign}[\mu]$ is observed, consequence of the arbitrary sign with which the T' coefficients can enter in most of the off-diagonal entries of the slepton mass matrices. As it can be noticed from the two upper plots, the low (A_0, m_0) scenario is almost excluded for both the cases: in the RP_A case mostly due to the requirement of neutral LSP, while in the RP_B case because of a too large BR. However, in the RP_B case few points are still allowed, independently of the $M_{1/2}$ value, thanks to a fine tuned cancellation between different terms. Concerning the $A_0 = 2m_0 = 2000$ GeV case, the left-lower plot of figure 3 shows that no constraints comes from the $\text{BR}(\mu \rightarrow e\gamma)$ for the RP_A scenario, while for large u and $\tan\beta$ (right-lower plot of figure 3) our T' model is allowed only for $M_{1/2} \gtrsim 500$ GeV. Our results are quite in agreement with the A_4 analysis of [60], once a factor 10 suppression in the BR, produced by the heavier spectrum, is taken into account. The results for the τ decays are not shown as no competing results are expected from $\tau \rightarrow e\gamma$ and $\tau \rightarrow \mu\gamma$ decays, even assuming Super B factory luminosities.

When studying FCNC, it is quite common to present bounds in terms of Mass Insertion (MI) instead of using directly the specific observables. The MI approach has the advantage to provide easy connections between the predictions of our T' model with the more general

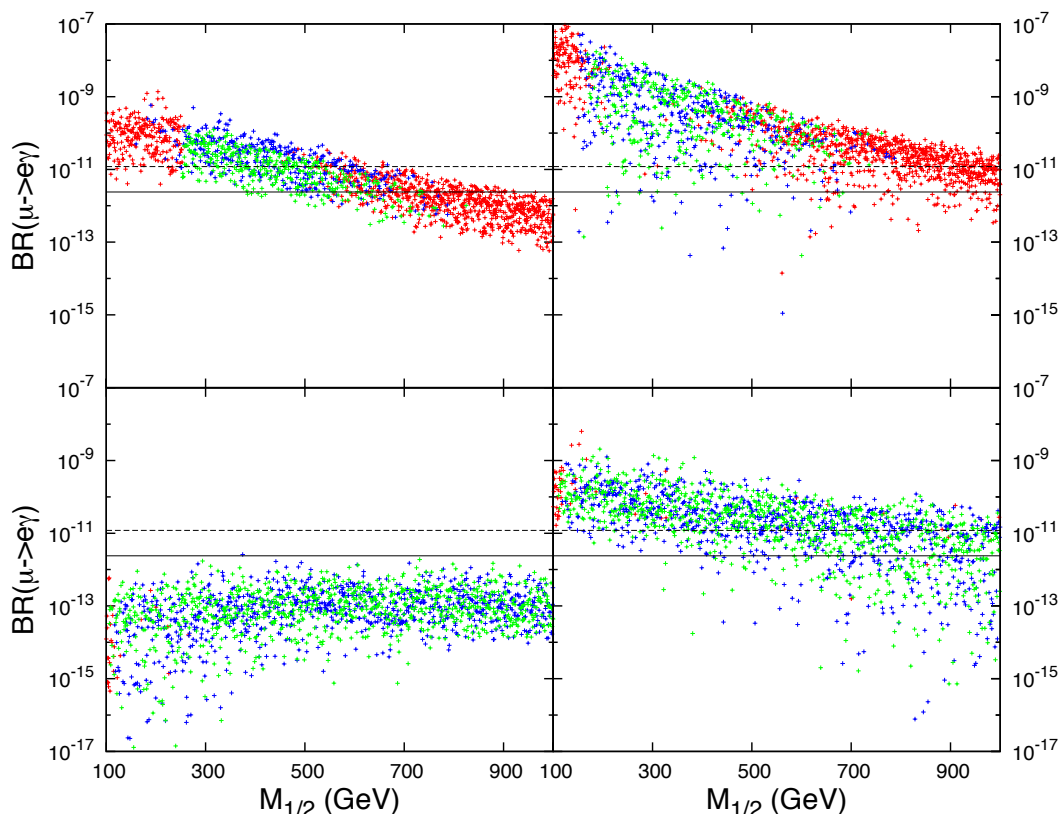


Figure 3. Scatter plots for $BR(\mu \rightarrow e\gamma)$ for the T' model. Red points are not allowed by “phenomenological” constraints on Higgs or SUSY masses. Blue (Green) points refer to $\mu > 0$ ($\mu < 0$). The full (dashed) line represents MEG (MEGA) bound. The left (right) plots refer to the RP_A (RP_B) case for $A_0 = 2m_0 = 400$ GeV (upper plots) or $A_0 = 2m_0 = 2000$ GeV (lower plots).

(SUSY) framework. We have not derived explicit formulas in the MI approximation as most of them can be found in [60]. Instead, a numerical analysis is performed and regions of expectation for all the MI have been derived.

A thoughtful work on leptonic MI in the SUSY context has been performed in [68], where the upper limits, in the single-dominance approximation, for all the relevant MIs are plotted as function of the scalar and gaugino common scales, $m_0, M_{1/2}$. To compare the results with the literature we have defined the MIs as the corresponding entry in the sfermion mass matrix divided by the “typical” SUSY scale that for being conservative we have chosen as the mass of the lightest scalar in the corresponding sector.

In figure 4 the results for the LL and RL leptonic MIs for the 21 sector, $(\delta^{21})_\ell$, are shown for the RP_A case and for the two reference values $A_0 = 2m_0 = 400$ GeV (upper plots) and $A_0 = 2m_0 = 2000$ GeV (lower plots). Dots represent the value of the relevant observable as computed (at one-loop in the NLO approximation) by SPheno as function of the SUSY gaugino parameter $M_{1/2}$ and varying randomly all the unknown T' coefficients in the $(1/2, 2)$ range. Orange points are excluded by present MEG bound on

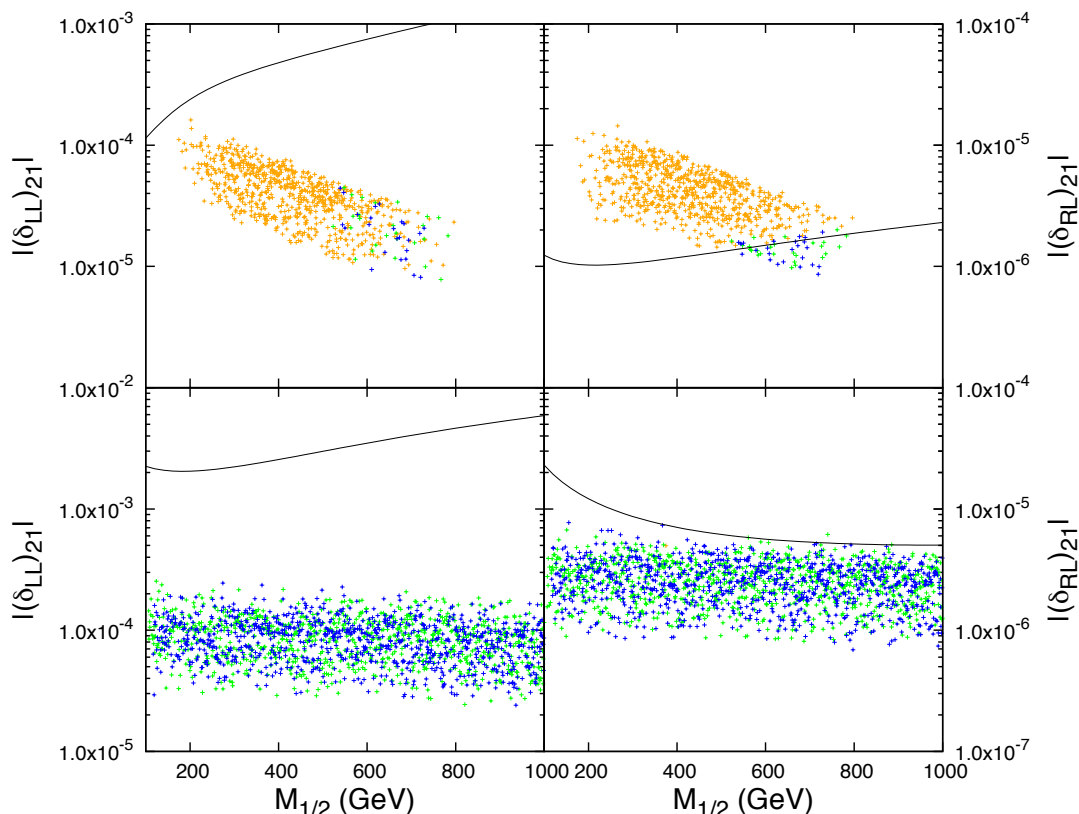


Figure 4. LL and RL Leptonic Mass insertions $(\delta^{21})_{\ell}$ for the RP_A case. In the upper (lower) plots $A_0 = 2m_0 = 400$ GeV ($A_0 = 2m_0 = 2000$ GeV) respectively. Orange points are not allowed by recent MEG data. Blue (Green) points refer to $\mu > 0$ ($\mu < 0$). Continuous lines represent MI bounds derived from ref. [68].

the $\mu \rightarrow e\gamma$ Branching Ratio, while Blue (Green) points represent an allowed region for $\mu > 0$ ($\mu < 0$) respectively. For all points shown, experimental spectrum constraints are satisfied. The continuous black lines represent the MI values, derived from ref. [68], that saturate the experimental data. As it can be noticed from the right-upper plot of figure 4, MEG data severely constrain our model and force the $(\delta_{RL}^{21})_{\ell}$ MI to be below 2×10^{-6} , with a mild dependence on $M_{1/2}$. This is, in fact, expected to be the dominant contribution in the low $\tan\beta$ regime. In our model the $(\delta_{LL}^{21})_{\ell}$ MI can vary in the range $10^{-5} - 10^{-4}$, roughly a factor 5-10 below the saturation limit. The RR and LR MIs are completely irrelevant in our analysis and therefore are not shown. When a higher value for the common scalar mass scale is chosen, $A_0 = 2m_0 = 2000$ GeV, no limits are obtained on the MIs, as shown in figure 4 (lower plots). The main contribution still comes from the $(\delta_{RL}^{21})_{\ell}$ MI, just below the saturation limit.

In figure 5 the results for the LL and RL leptonic MIs are shown for the RP_B case and for the two reference values $A_0 = 2m_0 = 400$ GeV (upper plots) and $A_0 = 2m_0 = 2000$ GeV (lower plots). As can be noticed, in this case the amount of flavour changing is too high

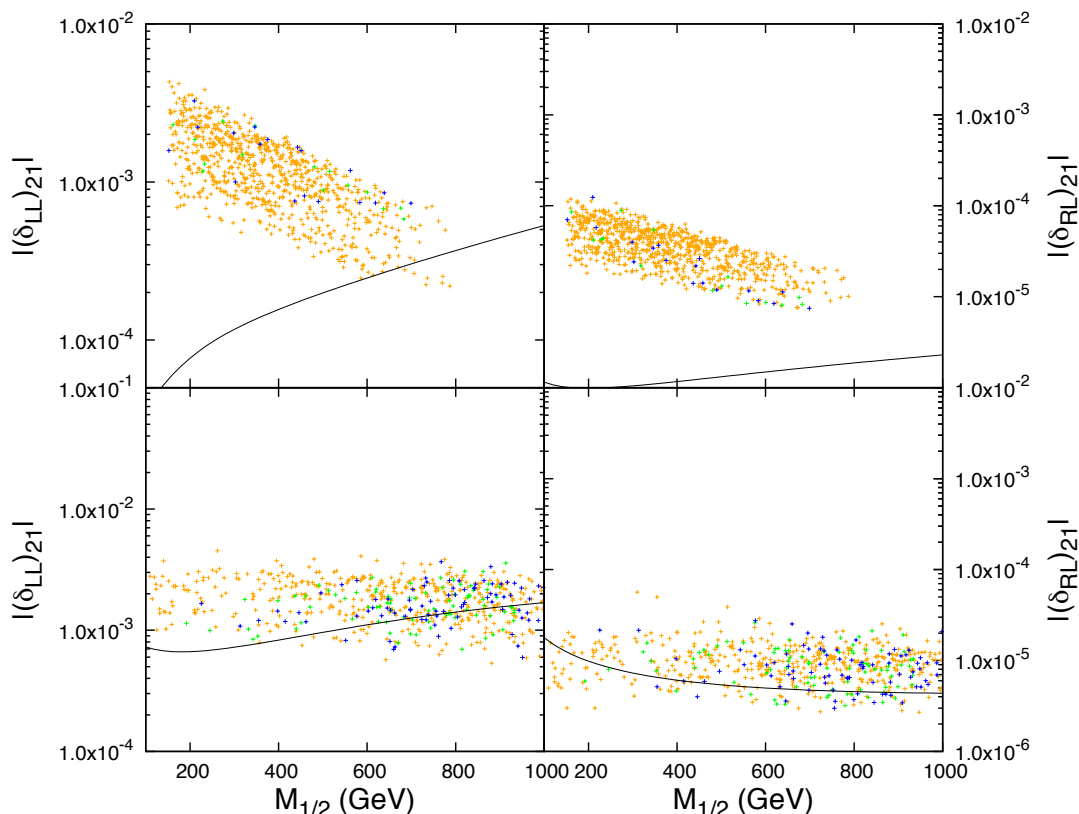


Figure 5. LL and RL Leptonic Mass insertions $(\delta^{21})_{\ell}$ for the RP_B case. In the upper (lower) plots $A_0 = 2m_0 = 400$ GeV ($A_0 = 2m_0 = 2000$ GeV) respectively. Orange points are not allowed by recent MEG data. Blue (Green) points refer to $\mu > 0$ ($\mu < 0$). Continuous lines represent MI bounds derived from ref. [68].

and, at least in the low scalar mass scale case (upper plots of figure 5), almost no points survive the experimental bound. Only at higher scalar scale the model is not completely excluded by MEG result, especially at high $M_{1/2}$ values. However, one expects that, for larger values of $\tan\beta$ as the one of RP_B , both LL and RL MIs can be relevant, opening the possibility of cancellations. This indeed happens in both low and high m_0 scenario, being particularly evident in the first case where even if both the LL and RL MIs are above the saturation limit of [68] by at least a factor 5-10, still few points of the model are allowed. Again the RR and LR MIs are completely irrelevant and therefore are not presented here.

The T' model at hands, predicts on the same footing also FCNC for the 31 and 32 MIs sectors. Bounds on $(\delta^{31})_{\ell}$ and $(\delta^{31})_{\ell}$ can be mostly obtained by analysing $\tau \rightarrow e\gamma$ and $\tau \rightarrow \mu\gamma$ radiative decays. Nevertheless, as already mentioned no relevant information come from these channels and these sectors are not shown here.

5.3 FCNC in the hadronic sector

Differently from the leptonic case, no previous study to the hadronic FCNC sector for the T' model as ever been performed before. Furthermore, for this sector no general MI analysis in all the available SUSY breaking parameters ($M_{1/2}$, m_0) has been performed, so we prefer to discuss the phenomenology directly showing the FCNC observables.

In order to study the hadronic FCNC observables, it has been necessary to modify the corresponding `SPheno` routines, and check the agreement with the literature in several ways [69, 70]. In the $b \rightarrow s\gamma$ Branching Ratio, new contributions coming from gluinos and neutralinos, not present in `SPheno-2.2.3`, have also been included [71]. Moreover as `SPheno` result is not completely up-to-date in reproducing the NNLO SM contribution to the $b \rightarrow s\gamma$ BR, we found more convenient to calculate with `SPheno` at NLO the “differential” Branching Ratio:

$$\Delta\text{BR}(\bar{B} \rightarrow X_s\gamma) = \text{BR}_{\text{SM+NP}}(\bar{B} \rightarrow X_s\gamma) - \text{BR}_{\text{SM}}(\bar{B} \rightarrow X_s\gamma).$$

We then compare it with the current experimental value [2], measured with a photon-energy cut-off $E_\gamma > 1.6 \text{ GeV}$ in the B -meson rest frame,

$$\text{BR}(\bar{B} \rightarrow X_s\gamma) = (3.55 \pm 0.24 \pm 0.09) \times 10^{-4},$$

subtracted by the SM prediction calculated at NNLO [72–74] for the same photon energy cut-off,

$$\text{BR}(\bar{B} \rightarrow X_s\gamma) = (3.15 \pm 0.23) \times 10^{-4}.$$

In figure 6 the T' Branching Ratio for $b \rightarrow s\gamma$ is shown as function of the common gaugino scale $M_{1/2}$. The two upper (lower) plots refer to $A_0 = 2m_0 = 400 \text{ GeV}$ ($A_0 = 2m_0 = 2000 \text{ GeV}$), respectively for the RP_A case (left) and RP_B case (right). Red points are excluded by imposing “phenomenological” requirements on the Higgs and/or SUSY masses. Blue (Green) points refer to $\mu > 0$ ($\mu < 0$) as usual. The horizontal dashed lines represent the 2σ experimental bound from ref. [2]. In the small (A_0, m_0) region (upper plots), the dominant T' contribution to the $b \rightarrow s\gamma$ BR is typically the charged Higgs one, due to the fact that the stop is for most of the $M_{1/2}$ range heavier than the H^\pm (and the chargino heavier than the top). The Higgs contribution is always concordant in sign with the SM one. The second most relevant contribution is the chargino one with a sign depending on $\text{sign}[\mu]$: it tends to enhance (cancel) the SM contribution for $\mu < 0$ ($\mu > 0$). Gluino contributions are practically independent from $\text{sign}[\mu]$, while neutralino ones are completely negligible. In appendix D, we report the break down of the relevant Wilson Coefficient for $\text{BR}(\bar{B} \rightarrow X_s\gamma)$ in terms of the supersymmetric contributions. This helps understanding the results showed in figure 6. As a consequence, experimental constraints on the $b \rightarrow s\gamma$ BR tend to disfavor $\mu < 0$ for $M_{1/2} \lesssim 500 \text{ GeV}$ especially for the larger $\tan\beta$ values of the RP_B point (right plots). The positive μ case, instead, turns out to be mostly allowed. In the $A_0 = 2m_0 = 2000 \text{ GeV}$ scenario (lower plots) all new physics contributions get strongly suppressed and no significative limits are expected from the $b \rightarrow s\gamma$ measurement in neither the two cases considered.

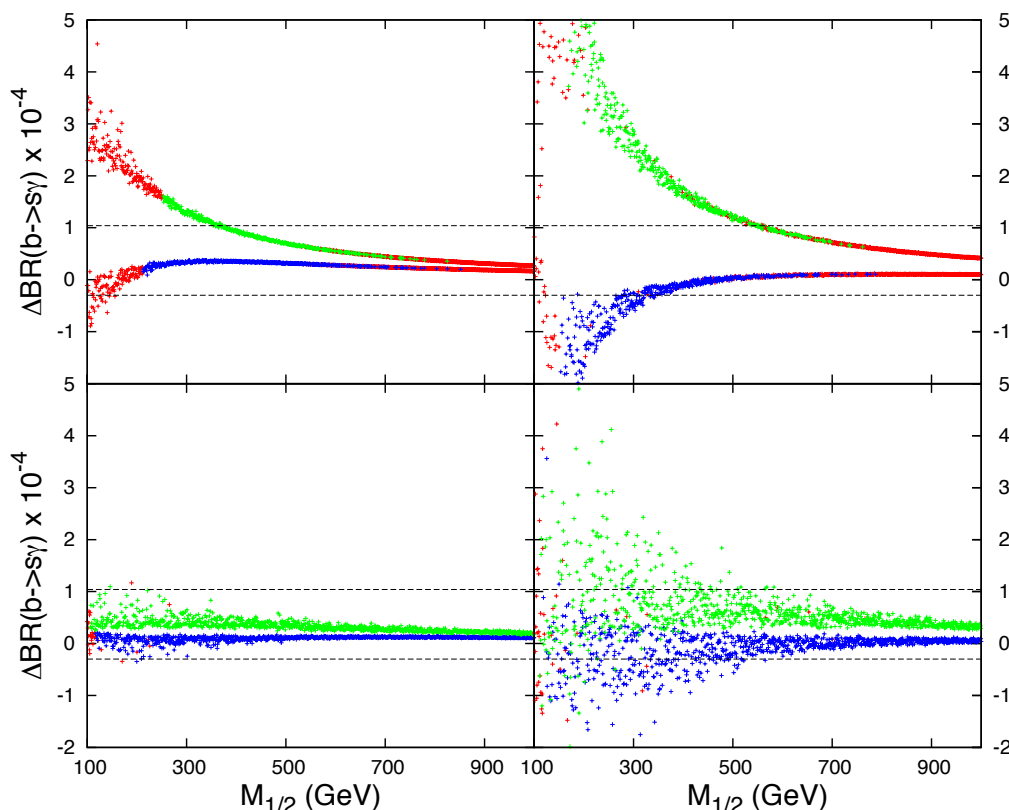


Figure 6. Scatter plots for the $b \rightarrow s\gamma$ BR for the T' model. Red points are not allowed by “phenomenological” constraints on Higgs or SUSY masses. Blue (Green) points refer to $\mu > 0$ ($\mu < 0$). The left (right) plots refer to the RP_A (RP_B) case for $A_0 = 2m_0 = 400$ GeV (upper plots) or $A_0 = 2m_0 = 2000$ GeV (lower plots).

In figure 7 the T' predictions for ΔM_{B_s} vs. ΔM_{B_d} are shown as function of the common gaugino mass $M_{1/2}$. The two upper (lower) plots refer to $A_0 = 2m_0 = 400$ GeV ($A_0 = 2m_0 = 2000$ GeV), respectively for the RP_A case (left) and RP_B case (right). Red points, as usual, are excluded by imposing “phenomenological” requirements on the Higgs and/or SUSY masses while Blue (Green) points refer to $\mu > 0$ ($\mu < 0$). The horizontal and vertical dashed lines show the 2σ bounds on the B_d and B_s mass differences obtained by ref. [75]:

$$\begin{aligned} \Delta M_{B_d} &= 0.55^{+0.11}_{-0.10} \text{ ps}^{-1} \\ \Delta M_{B_s} &= 16.8^{+4.1}_{-2.8} \text{ ps}^{-1}, \end{aligned}$$

perfectly compatible with present experimental bounds from ref. [2]:

$$\begin{aligned} \Delta M_{B_d} &= 0.507 \pm 0.005 \text{ ps}^{-1} \\ \Delta M_{B_s} &= 17.77 \pm 0.12 \text{ ps}^{-1}. \end{aligned}$$

The T' SUSY contribution to $\Delta M_{B_{d,s}}$ has always opposite sign compared to the SM one, independently on the sign $[\mu]$. As evident from the plots of figure 7 this fact always leads

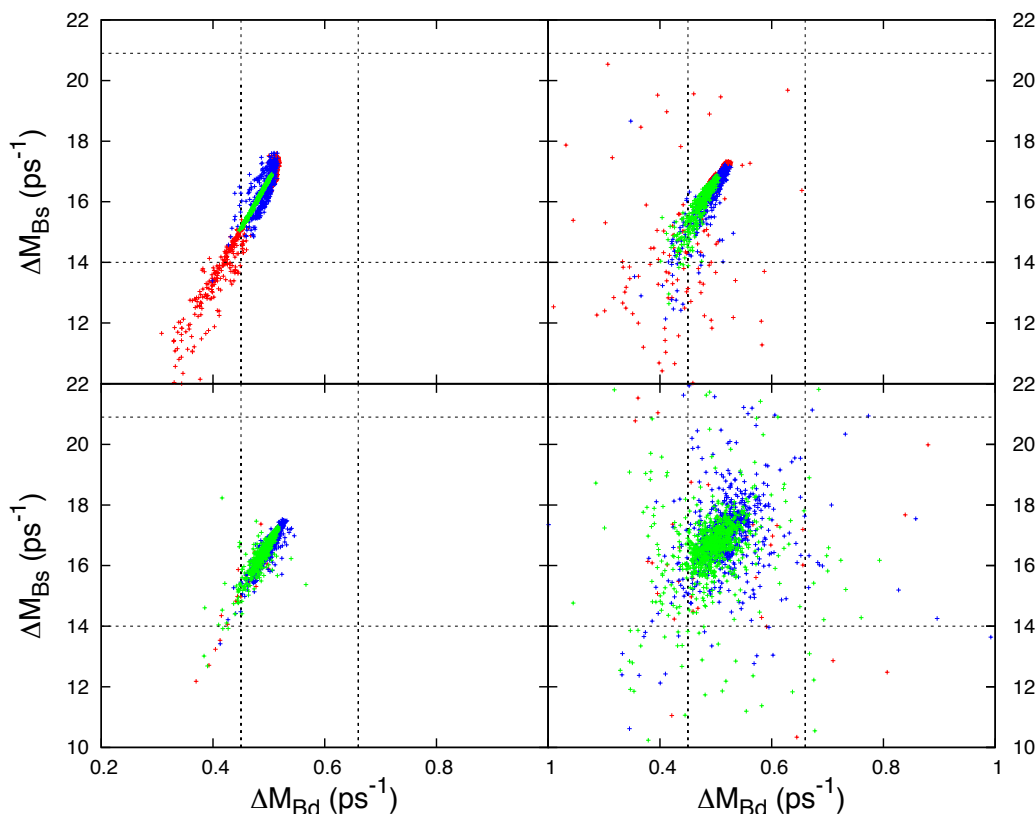


Figure 7. Scatter plots for ΔM_{B_s} vs. ΔM_{B_d} for the T' model. Red points are not allowed by “phenomenological” constraints on Higgs or SUSY masses. Blue (Green) points refer to $\mu > 0$ ($\mu < 0$). The dashed lines represent 2σ experimental bound. The left (right) plots refer to the RP_A (RP_B) case for $A_0 = 2m_0 = 400$ GeV (upper plots) or $A_0 = 2m_0 = 2000$ GeV (lower plots).

to a suppression of the neutral meson mass differences, where the “comet” tail is obtained for large values of $M_{1/2}$, while for small $M_{1/2}$ the points addensate in the “comet” head region. However, both B_d and B_s bounds are still too loose to provide any useful constraints especially in the RP_A scenario (left plots). Nevertheless it is interesting to note that, for the higher $\tan \beta$ of the RP_B scenario (right plots) the low $M_{1/2}$, tails start getting excluded by the present value of ΔM_{B_d} both in the low and in the high m_0 case. One can expect, that with a future improvement in the hadronic flavour parameters at LHCb or at Super B factories, constraints from the hadronic FCNC will start being competitive with the leptonic experiments.

Finally, no relevant bounds from $K^0 - \bar{K}^0$ oscillations are obtained in our model as the first two family squarks are nearly degenerate, producing no significant deviations from the SM (though poorly known) reference value.

5.4 Cross-correlations between leptonic and hadronic observables

The main feature of the SUSY T' model presented in this paper is the simultaneous prediction of the SM fermion mass sector together with the sfermion mass matrix structures. Furthermore, the amount of FCNC in the leptonic and hadronic sectors are tightly connected, providing very peculiar signatures.

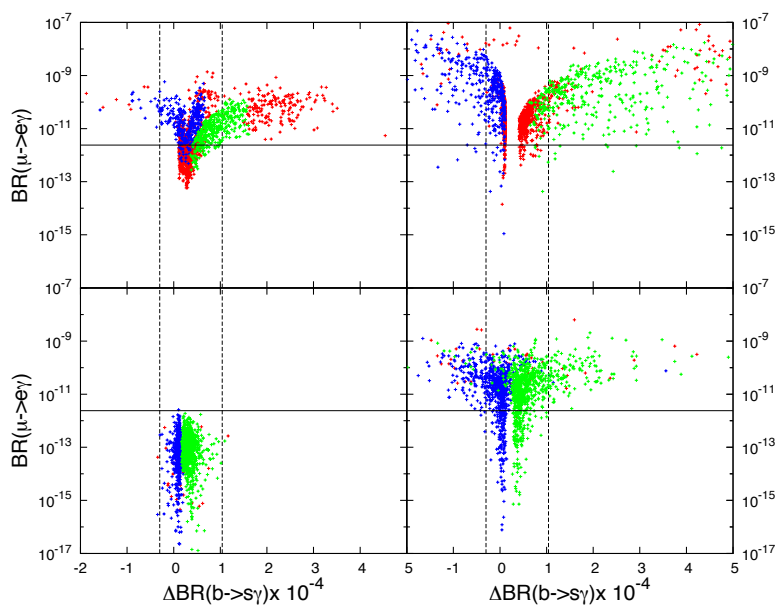
In figure 8 the T' cross-correlations between $\mu \rightarrow e\gamma$ vs. $b \rightarrow s\gamma$ (figure 8(a)) and $\mu \rightarrow e\gamma$ vs. ΔM_{B_d} (figure 8(b)) are shown varying the common gaugino mass $M_{1/2}$ in the range (100, 1000) GeV. The left (right) plots refer to the RP_A (RP_B) case, while in the upper (lower) plots of each figure the $A_0 = 2m_0 = 400$ GeV ($A_0 = 2m_0 = 2000$ GeV) case is presented. Red points are excluded by imposing “phenomenological” requirements on the Higgs and/or SUSY masses. Blue (Green) points refer to $\mu > 0$ ($\mu < 0$) as usual. The horizontal dashed lines indicate the 2σ experimental bounds as reported in the previous subsections.

It is evident from figure 8(a) that the strongest constraint still comes from the $\mu \rightarrow e\gamma$ BR, which almost excludes the small m_0 region. However, when larger values of m_0 are considered (lower plots), an improvement in the $\mu \rightarrow e\gamma$ bound will not impose any severe exclusion on the model, as BR values as small as 10^{-15} are still acceptable. Some help can come, instead, from the hadronic sector. For the moment the precision in the $b \rightarrow s\gamma$ BR measurement is not sufficiently good to impose further bounds on the T' model, when larger values of m_0 are considered (lower plots). However, an improved measure of $b \rightarrow s\gamma$, can eventually leads in the large $\tan\beta$ scenario to a discrimination of the sign $[\mu]$. An improvement in the knowledge of the meson mass differences at future facilities can help in further constraining the model in the large $\tan\beta$ regime (see lower-right plot of figure 8(b)), while the large m_0 , small $\tan\beta$ case will be almost impossible to exclude.

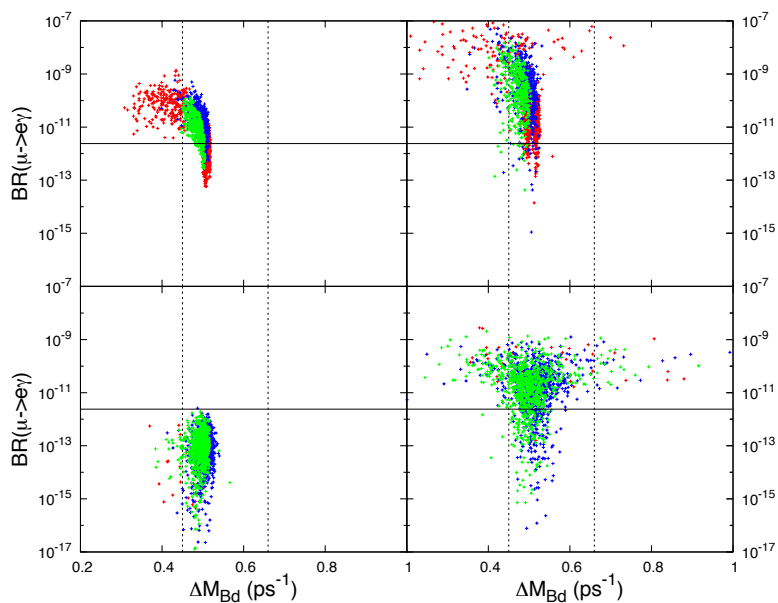
6 Conclusions

In the Standard Model (SM) of particle physics an explanation of the origin of the fermionic mass and mixing patterns is missing. A complete description of Nature should include a comprehensive description of the flavour sector. In this paper, a SUSY model based on the discrete flavour group T' , mainly based on ref. [1], has been analysed. This model accounts both for leptons, predicting the TB mixing pattern, and for quarks, providing a realistic CKM matrix.

While several flavour models can accomplish these goals, however, a discrimination between them can only be obtained through a detailed analysis of the associated phenomenology. In this paper we have studied the T' model predictions to the most relevant, leptonic and hadronic, FCNC observables. Concerning the leptonic FCNC we have essentially confirmed the $\mu \rightarrow e\gamma$ results obtained in ref. [60] for the A_4 model, as the two realisations (almost) coincide when restricted to leptons. The main difference is related to the full implementation in our study of the RGE for the low energy SUSY spectrum, by means of the use of the **SPheno** routines. In addition we performed, for the first time, a detailed analysis of the T' predictions for FCNC in the hadronic sector. It turns out that the amount of FCNC in the leptonic and hadronic sectors are tightly connected.



(a) Scatter plots for $\mu \rightarrow e\gamma$ vs. $b \rightarrow s\gamma$ for the T' model. The left (right) plots refer to the RP_A (RP_B) case respectively for $A_0 = 2m_0 = 400$ GeV (upper plots) or $A_0 = 2m_0 = 2000$ GeV (bottom plots).



(b) Scatter plots for $\mu \rightarrow e\gamma$ vs. ΔM_{B_d} for the T' model. The left (right) plots refer to the RP_A (RP_B) case respectively for $A_0 = 2m_0 = 400$ GeV (upper plots) or $A_0 = 2m_0 = 2000$ GeV (bottom plots).

Figure 8. Cross correlations between hadronic and leptonic observables. Red points are not allowed by “phenomenological” requirements on Higgs and/or SUSY masses. Blue (Green) points refer to $\mu > 0$ ($\mu < 0$).

The strongest bounds on the FCNC sector still come from the $\mu \rightarrow e\gamma$ Branching Ratio. Making use of the latest available MEG data, supplemented by “phenomenological” constraints on the Higgs and SUSY spectrum, almost all the available parameter space is excluded in the low (A_0, m_0) region. No bounds can be set when the common soft scalar breaking scale is increased to the TeV range and small values of the T' symmetry breaking parameter u are selected, while the low $M_{1/2}$ region is excluded for larger u and $\tan\beta$. Hadronic FCNC observables like $b \rightarrow s\gamma$ Branching Ratio or the neutral B meson mass differences, ΔM_{B_d} and ΔM_{B_s} can provide independent information, even if they are not yet enough precise to severely constrain the model. A factor 2 improvement in their experimental and theoretical determinations could however be enough for making the corresponding constraints quite competitive. The neutral K meson mass difference, ΔM_K turns out to almost coincide with SM prediction, due to the quasi degeneracy in the first two squark families.

The forthcoming results from LHCb and Super B factories will provide stronger constraints in the hadronic sector and allow a better study of the parameter space for the T' model.

Acknowledgments

The authors thanks A. Casas, M. E. Cabrera, F. Feruglio and P. Paradisi for very useful discussions. L. Merlo and B. Zaldívar Montero thank the Dipartimento di Fisica “Galileo Galilei” of the Università degli Studi di Padova for hospitality during the development of this project. L. Merlo and S. Rigolin thank the Departamento de Física Teórica of the Universidad Autónoma de Madrid for hospitality during the development of this project. L. Merlo acknowledges the German Bundesministerium für Bildung und Forschung’ under contract 05H09WOE. S. Rigolin acknowledges the partial support of an Excellence Grant of Fondazione Cariparo and of the European Program, Unification in the LHC era, under the contract PITN- GA-2009-237920 (UNILHC). B. Zaldívar Montero acknowledges the financial support of the FPI (MICINN) grant BES-2008-004688, and the contracts FPA2010-17747 and PITN-GA-2009-237920 (UNILHC) of the European Commission.

A The group T'

The group T' has 24 elements and 7 irreducible representations: one triplet $\mathbf{3}$, three doublets $\mathbf{2}$, $\mathbf{2}'$ and $\mathbf{2}''$ and three singlets $\mathbf{1}$, $\mathbf{1}'$ and $\mathbf{1}''$. It is generated by two elements S and T fulfilling the relations

$$S^2 = \mathbb{R}, \quad T^3 = \mathbb{1}, \quad (ST)^3 = \mathbb{1}, \quad \mathbb{R}^2 = \mathbb{1}, \quad (\text{A.1})$$

where $\mathbb{R} = \mathbb{1}$ in case of the odd-dimensional representation and $\mathbb{R} = -\mathbb{1}$ for $\mathbf{2}$, $\mathbf{2}'$ and $\mathbf{2}''$ such that \mathbb{R} commutes with all elements of the group. Beyond the center of the group, generated by the elements $\mathbb{1}$ and \mathbb{R} , there are other Abelian subgroups: Z_3 , Z_4 and Z_6 . In particular, there is a Z_4 subgroup here denoted by G_S , generated by the element TST^2

and a Z_3 subgroup here called G_T , generated by the element T . G_S and G_T are of great importance because they represent the low-energy flavour structures of the fermion masses.

The multiplication rules of the representations are as follows:

$$\begin{aligned}
 \mathbf{1}^a \times \mathbf{r}^b &= \mathbf{r}^b \times \mathbf{1}^a = \mathbf{r}^{a+b} && \text{for } \mathbf{r} = \mathbf{1}, \mathbf{2} \\
 \mathbf{1}^a \times \mathbf{3} &= \mathbf{3} + \mathbf{1}^a = \mathbf{3} \\
 \mathbf{2}^a \times \mathbf{2}^b &= \mathbf{3} + \mathbf{1}^{a+b} \\
 \mathbf{2}^a \times \mathbf{3} &= \mathbf{3} \times \mathbf{2}^a = \mathbf{2} + \mathbf{2}' + \mathbf{2}'' \\
 \mathbf{3} \times \mathbf{3} &= \mathbf{3} + \mathbf{3} + \mathbf{1} + \mathbf{1}' + \mathbf{1}''
 \end{aligned}
 \tag{A.2}$$

where $a, b = 0, \pm 1$ and we have denoted $\mathbf{1}^0 \equiv \mathbf{1}$, $\mathbf{1}^1 \equiv \mathbf{1}'$, $\mathbf{1}^{-1} \equiv \mathbf{1}''$ and similarly for the doublet representations. On the right-hand side the sum $a + b$ is modulo 3. The Clebsch-Gordan coefficients for the decomposition of product representations can be found in ref. [1].

B Details on the sfermion mass matrices

In this appendix we give more details on the computation of the sfermion mass matrices listed in the sections 3.3 and 4.

The contributions to the sfermion masses from the SUSY breaking terms in the Kähler potential are given by two distinct terms: $(m_{fLL}^2)_K$ of eqs. (3.46)–(3.50) and those contributions related to the non-vanishing VEV of the auxiliary fields of the flavon supermultiplets. Denoting these second ones as $(m_{fLL}^2)_{K2}$, we find for the slepton sector:

$$(m_{(e,\nu)LL}^2)_{K2} = \begin{pmatrix} t_{F1}^\ell & u^2 & t_{F4}^\ell & u^2 & t_{F5}^\ell & u^2 \\ \bar{t}_{F4}^\ell & u^2 & t_{F2}^\ell & u^2 & t_{F6}^\ell & u^2 \\ \bar{t}_{F5}^\ell & u^2 & \bar{t}_{F6}^\ell & u^2 & t_{F3}^\ell & u^2 \end{pmatrix}, \tag{B.1}$$

$$(m_{eRR}^2)_{K2} = \begin{pmatrix} t_{F1}^e & u^2 & t_{F4}^e & u^2 t & t_{F5}^e & u^2 t^2 \\ \bar{t}_{F4}^e & u^2 t & t_{F2}^e & u^2 & t_{F6}^e & u^2 t \\ \bar{t}_{F5}^e & u^2 t^2 & \bar{t}_{F6}^e & u^2 t & t_{F3}^e & u^2 \end{pmatrix}, \tag{B.2}$$

where the coefficients $t_F^{\ell,e}$ are combinations of p_I in eq. (3.16) and the distinct c_F in eqs. (2.10). Such relations are not particularly significant and we avoid to report them here. Notice that these contributions are absent in ref. [60], but do not change those results: indeed $(m_{eLL}^2)_{K2}$, $(m_{\nu LL}^2)_{K2}$ and $(m_{eRR}^2)_{K2}$ can be safely absorbed in a redefinition of the parameters of $(m_{eLL}^2)_K$, $(m_{\nu LL}^2)_K$ and $(m_{eRR}^2)_K$.

For the same contributions in the quark sector we get:

$$(m_{(u,d)LL}^2)_{K2} = \begin{pmatrix} t_{F1}^q & u^2 & t_{F4}^q & u^2 & t_{F5}^q & u^2 \\ \bar{t}_{F4}^q & u^2 & t_{F2}^q & u^2 & t_{F6}^q & u^2 \\ \bar{t}_{F5}^q & u^2 & \bar{t}_{F6}^q & u^2 & t_{F3}^q & u^2 \end{pmatrix}, \quad (\text{B.3})$$

$$(m_{uRR}^2)_{K2} = \begin{pmatrix} t_{F1}^u & u^2 & t_{F5}^u & u^2 & t_{F6}^u & u^2 \\ \bar{t}_{F5}^u & u^2 & t_{F2}^u & u^2 & t_{F4}^u & u^2 \\ \bar{t}_{F6}^u & u^2 & \bar{t}_{F4}^u & u^2 & t_{F2}^u & u^2 \end{pmatrix}, \quad (\text{B.4})$$

$$(m_{dRR}^2)_{K2} = \begin{pmatrix} t_{F1}^d & u^2 & t_{F4}^d & u^2 & t_{F5}^d & u^2 \\ \bar{t}_{F4}^d & u^2 & t_{F2}^d & u^2 & t_{F6}^d & u^2 \\ \bar{t}_{F5}^d & u^2 & \bar{t}_{F6}^d & u^2 & t_{F3}^d & u^2 \end{pmatrix}, \quad (\text{B.5})$$

where the coefficients $t_F^{q,u,d}$ are combinations of p_I in eq. (3.16) and the distinct c_F in eqs. (2.10). Such relations are not particularly significant. Furthermore notice that $(m_{uLL}^2)_{K2}$, $(m_{dLL}^2)_{K2}$, $(m_{uRR}^2)_{K2}$ and $(m_{dRR}^2)_{K2}$ can be safely absorbed in a redefinition of the parameters in $(m_{uLL}^2)_K$, $(m_{dLL}^2)_K$, $(m_{uRR}^2)_K$ and $(m_{dRR}^2)_K$.

We then comment on additional SUSY contributions to the m_{fRR}^2 mass matrices coming from the D terms. The relevant factors in the scalar potential (through a D term) are the following:

$$\begin{aligned} V_{D,\text{FN}} &= \frac{1}{2} \left(M_{\text{FI}}^2 + g_{\text{FN}} Q_{\text{FN}}^i \frac{\partial \mathcal{K}}{\partial \phi_i} \phi_i \right)^2 + g_{\text{FN}} m_0^2 |\theta_{\text{FN}}|^2 \\ &= g_{\text{FN}}^2 c_\theta m_0^2 \left[2|\tilde{e}^c|^2 + |\tilde{\mu}^c|^2 + |\tilde{u}^c|^2 + |\tilde{c}^c|^2 + |\tilde{d}^c|^2 + |\tilde{s}^c|^2 + |\tilde{b}^c|^2 + \right. \\ &\quad \left. + (t_4^e u^2 t \bar{e}^c \tilde{\mu}^c + t_6^e u^2 t \bar{\mu}^c \tilde{\tau}^c + t_6^u u t \bar{u}^c \tilde{t}^c + \text{h.c.}) \right] + \dots \end{aligned} \quad (\text{B.6})$$

where Q_{FN}^i stands for the FN charge of the scalar field ϕ_i , and in the second line we have displayed only the leading contributions to the terms quadratic in the matter fields for the slepton and the squark sectors. This result has been recovered considering the FN field vevs in eq. (3.41), but in the SUSY broken phase:

$$\frac{M_{\text{FI}}^2}{g_{\text{FN}}} - |\langle \theta_{\text{FN}} \rangle|^2 = c_\theta m_0^2. \quad (\text{B.7})$$

As commented in section 3.3, these contributions can be simply reabsorbed in $(m_{fRR}^2)_K$ through a field redefinition.

Once in the physical basis and assuming for simplicity that all the parameters of the model are real, we find the following results for the sfermion mass matrices.

We start with the LL block. For the sleptons we find

$$(\hat{m}_{(e,\nu)LL}^2)_K = \begin{pmatrix} n_0^\ell + 2\hat{n}_1^\ell u & \hat{n}_4^\ell u^2 & (\hat{n}_5^\ell + (3\hat{n}_1^\ell - \hat{n}_2^\ell)c_{T3})u^2 \\ \hat{n}_4^\ell u^2 & n_0^\ell - (\hat{n}_1^\ell + \hat{n}_2^\ell)u & \hat{n}_6^\ell u^2 \\ (\hat{n}_5^\ell + (3\hat{n}_1^\ell - \hat{n}_2^\ell)c_{T3})u^2 & \hat{n}_6^\ell u^2 & n_0^\ell - (\hat{n}_1^\ell - \hat{n}_2^\ell)u \end{pmatrix} m_0^2, \quad (\text{B.8})$$

where the coefficients are defined by

$$\hat{n}_i^\ell = n_i^\ell - t_i^\ell n_0^\ell \quad (i = 1, 2, 4, 5, 6). \quad (\text{B.9})$$

For the squarks we have

$$(\hat{m}_{(u,d)LL}^2)_K = \begin{pmatrix} \hat{n}_0^q - \hat{n}_2^q u & 2c'' \hat{n}_2^q \frac{\tilde{y}_6}{y_5} u \sqrt{t} & c'' \hat{n}_3^q \frac{\tilde{y}_6}{y_5} u \sqrt{t} \\ 2c'' \hat{n}_2^q \frac{\tilde{y}_6}{y_5} u \sqrt{t} & \hat{n}_0^q + \hat{n}_2^q u & \hat{n}_3^q u \\ c'' \hat{n}_3^q \frac{\tilde{y}_6}{y_5} u \sqrt{t} & \hat{n}_3^q u & \hat{n}_1^q \end{pmatrix} m_0^2, \quad (\text{B.10})$$

where the coefficients are defined by

$$\begin{aligned} \hat{n}_0^q &= \frac{n_0^q}{t_d^q}, & \hat{n}_1^q &= \frac{n_1^q}{t_s^q}, & \hat{n}_2^q &= \frac{1}{t_d^q} (n_2^q - t_1^q \hat{n}_0^q), \\ \hat{n}_3^q &= \frac{1}{\sqrt{t_s^q t_d^q}} (n_4^q - t_4^q \hat{n}_0^q) + c' \frac{y_7}{y_b} \sqrt{\frac{t_s^q}{t_d^q}} (\hat{n}_0^q - \hat{n}_1^q). \end{aligned} \quad (\text{B.11})$$

For the RR block we find that $(\hat{m}_{fRR}^2)_K$ for the sleptons is given by

$$(\hat{m}_{eRR}^2)_K = \begin{pmatrix} n_1^c & 2c_{T3} (n_1^c - n_2^c) \frac{m_e}{m_\mu} u & 2c_{T3} (n_1^c - n_3^c) \frac{m_e}{m_\tau} u \\ 2c_{T3} (n_1^c - n_2^c) \frac{m_e}{m_\mu} u & n_2^c & 2c_{T3} (n_2^c - n_3^c) \frac{m_\mu}{m_\tau} u \\ 2c_{T3} (n_1^c - n_3^c) \frac{m_e}{m_\tau} u & 2c_{T3} (n_2^c - n_3^c) \frac{m_\mu}{m_\tau} u & n_3^c \end{pmatrix} m_0^2, \quad (\text{B.12})$$

while for the up squarks we have

$$(\hat{m}_{uRR}^2)_K = \begin{pmatrix} \hat{n}_0^u - \hat{n}_2^u u & \hat{n}_5^u u^2 & \hat{n}_6^u t u^2 \\ \hat{n}_5^u u^2 & \hat{n}_0^u + \hat{n}_2^u u & \hat{n}_4^u t u \\ \hat{n}_6^u t u^2 & \hat{n}_4^u t u & \hat{n}_1^u \end{pmatrix} m_0^2, \quad (\text{B.13})$$

where the coefficients are defined by

$$\begin{aligned} \hat{n}_0^u &= \frac{n_0^u}{t_d^u}, & \hat{n}_1^u &= \frac{n_1^u}{t_s^u}, & \hat{n}_2^u &= \frac{1}{t_d^u} (n_2^u - t_1^u \hat{n}_0^u), \\ \hat{n}_4^u &= \frac{1}{\sqrt{t_d^u t_s^u}} \left(n_4^u - t_4^u \frac{n_0^u - n_1^u}{t_d^u - t_s^u} \right), & \hat{n}_5^u &= \frac{1}{t_d^u} \left(n_5^u - \frac{t_5^u}{t_1^u} n_2^u \right), \\ \hat{n}_6^u &= \frac{1}{\sqrt{t_d^u t_s^u}} \left(n_6^u - t_6^u \frac{n_0^u - n_1^u}{t_d^u - t_s^u} \right) - \frac{t_5^u}{2t_1^u} \hat{n}_4^u, \end{aligned} \quad (\text{B.14})$$

and finally for the down squarks we get

$$(\hat{m}_{dRR}^2)_K = \begin{pmatrix} n_0^d - \hat{n}_2^d u & -2c'' \hat{n}_2^d \frac{\tilde{y}_6}{y_5} u \sqrt{t} & -c'' \hat{n}_3^d \frac{\tilde{y}_6}{y_5} u \sqrt{t} \\ -2c'' \hat{n}_2^d \frac{\tilde{y}_6}{y_5} u \sqrt{t} & n_0^d + \hat{n}_2^d u & \hat{n}_3^d u \\ -c'' \hat{n}_3^d \frac{\tilde{y}_6}{y_5} u \sqrt{t} & \hat{n}_3^d u & n_1^d \end{pmatrix} m_0^2, \quad (\text{B.15})$$

with the coefficients given by

$$\begin{aligned}\hat{n}_0^d &= \frac{n_0^d}{t_d^d}, & \hat{n}_1^d &= \frac{n_1^d}{t_s^d}, & \hat{n}_2^d &= \frac{1}{t_d^d} \left(n_2^d - t_s^d \hat{n}_0^d \right), \\ \hat{n}_3^d &= \frac{1}{\sqrt{t_s^d t_d^d}} \left(n_4^d - t_4^d \hat{n}_0^d \right) + c' \frac{y_8}{y_b} \sqrt{\frac{t_s^d}{t_d^d}} \left(\hat{n}_0^d - \hat{n}_1^d \right).\end{aligned}\tag{B.16}$$

Finally, we report the results for the RL block. For the charged sleptons, the contributions are the following:

$$\left(\hat{m}_{eRL}^2 \right)_1 = \hat{A}_1^e \frac{v \cos \beta}{\sqrt{2}} A_0, \quad \left(\hat{m}_{eRL}^2 \right)_2 = \hat{A}_2^e \frac{v \cos \beta}{\sqrt{2}} A_0,\tag{B.17}$$

where \hat{A}_1^e is given by

$$\begin{aligned}\left[\hat{A}_1^e \right]_{11} &= \frac{z_e}{y_e} m_e \frac{\sqrt{2}}{v \cos \beta}, \\ \left[\hat{A}_1^e \right]_{12} &= c_{T3} \frac{(z_e y_\mu - z_\mu y_e)}{y_e y_\mu} m_e u \frac{\sqrt{2}}{v \cos \beta}, \\ \left[\hat{A}_1^e \right]_{13} &= c_{T3} \frac{(z_e y_\tau - z_\tau y_e)}{y_e y_\tau} m_e u \frac{\sqrt{2}}{v \cos \beta}, \\ \left[\hat{A}_1^e \right]_{21} &= \left[c_{T2} \frac{(z_\mu y'_\mu - z'_\mu y_\mu)}{y_\mu^2} m_\mu t u^2 + c_{T3} \frac{(z_e y_\mu - z_\mu y_e)}{y_\mu^2} m_e t u + \right. \\ &\quad \left. - c_{T3} \left(\frac{(z_\mu y'_\mu - z'_\mu y_\mu)}{y_\mu^2} + \frac{(z_\tau y'_\tau - z'_\tau y_\tau)}{y_\tau^2} \right) m_\mu u^3 \right] \frac{\sqrt{2}}{v \cos \beta}, \\ \left[\hat{A}_1^e \right]_{22} &= \frac{z_\mu}{y_\mu} m_\mu \frac{\sqrt{2}}{v \cos \beta}, \\ \left[\hat{A}_1^e \right]_{23} &= c_{T3} \frac{(z_\mu y_\tau - z_\tau y_\mu)}{y_\mu y_\tau} m_\mu u \frac{\sqrt{2}}{v \cos \beta}, \\ \left[\hat{A}_1^e \right]_{31} &= c_{T3} \frac{(z_\tau y'_\tau - z'_\tau y_\tau)}{y_\tau^2} m_\tau u^2 \frac{\sqrt{2}}{v \cos \beta}, \\ \left[\hat{A}_1^e \right]_{32} &= \left[c_{T2} \frac{(z_\tau y'_\tau - z'_\tau y_\tau)}{y_\tau^2} m_\tau t u^2 + c_{T3} \frac{(z_\mu y_\tau - z_\tau y_\mu)}{y_\tau^2} m_\mu t u \right] \frac{\sqrt{2}}{v \cos \beta}, \\ \left[\hat{A}_1^e \right]_{33} &= \frac{z_\tau}{y_\tau} m_\tau \frac{\sqrt{2}}{v \cos \beta},\end{aligned}\tag{B.18}$$

while for \hat{A}_2^e we have

$$\hat{A}_2^e = \begin{pmatrix} c^F m_e & (c_{T3}^F - c^F c_{T3}) m_e u & c_{T2}^F m_e u \\ c_{T2}^F m_\mu u & c^F m_\mu & (c_{T3}^F - c^F c_{T3}) m_\mu u \\ (c_{T3}^F - c^F c_{T3}) m_\tau u & c_{T2}^F m_\tau u & c^F m_\tau \end{pmatrix} \frac{\sqrt{2}}{v \cos \beta},\tag{B.19}$$

Moving to the up squarks, the contributions are the following:

$$\left(\hat{m}_{uRL}^2 \right)_1 = \hat{A}_1^u \frac{v \sin \beta}{\sqrt{2}} A_0, \quad \left(\hat{m}_{uRL}^2 \right)_2 = \hat{A}_2^u \frac{v \sin \beta}{\sqrt{2}} A_0,\tag{B.20}$$

where \hat{A}_1^u is given by

$$\begin{aligned}
\left[\hat{A}_1^u\right]_{11} &= \frac{c'' \tilde{y}_6}{y_5} \left[\left(\frac{c_{T3} z_1 + 2c'' z_2}{2\sqrt{t_d^q t_d^u}} - \frac{t_5^u z_1}{2\sqrt{t_d^q t_d^u t_1^u}} + \frac{c' t_6^u (z_3 y_b - z_t y_7)}{\sqrt{t_d^q t_d^u (t_d^u - t_s^u) y_b}} \right) \sqrt{t} u^3 + \right. \\
&\quad \left. - \frac{c' t_4^u t_5^u (z_3 y_b - z_t y_7)}{2\sqrt{t_d^q t_d^u t_1^u (t_d^u - t_s^u) y_b}} \frac{u^4}{\sqrt{t}} \right], \\
\left[\hat{A}_1^u\right]_{12} &= \left(\frac{c_{T3} z_1 + 2c'' z_2}{2\sqrt{t_d^q t_d^u}} - \frac{t_5^u z_1}{2\sqrt{t_d^q t_d^u t_1^u}} + \frac{c' t_6^u (z_3 y_b - z_t y_7)}{\sqrt{t_d^q t_d^u (t_d^u - t_s^u) y_b}} \right) t u^2 + \\
&\quad - \frac{c' t_4^u t_5^u (z_3 y_b - z_t y_7)}{2\sqrt{t_d^q t_d^u t_1^u (t_d^u - t_s^u) y_b}} u^3, \\
\left[\hat{A}_1^u\right]_{13} &= \frac{t_6^u z_t}{\sqrt{t_s^q t_d^u (t_d^u - t_s^u)}} t u - \frac{t_4^u t_5^u z_t}{2\sqrt{t_s^q t_d^u t_1^u (t_d^u - t_s^u)}} u^2, \\
\left[\hat{A}_1^u\right]_{21} &= \frac{c'' z_1 \tilde{y}_6}{\sqrt{t_d^q t_d^u} y_5} \sqrt{t} u^2 + \frac{c' t_4^u (z_3 y_b - z_t y_7)}{\sqrt{t_d^q t_d^u (t_d^u - t_s^u) y_5 y_b}} \frac{u^3}{\sqrt{t}} \\
\left[\hat{A}_1^u\right]_{22} &= \frac{z_1}{\sqrt{t_d^q t_d^u}} t u + \frac{c' t_4^u (z_3 y_b - z_t y_7)}{\sqrt{t_d^q t_d^u (t_d^u - t_s^u) y_b}} u^2, \\
\left[\hat{A}_1^u\right]_{23} &= \frac{t_4^u z_t}{\sqrt{t_s^q t_d^u (t_d^u - t_s^u)}} u, \\
\left[\hat{A}_1^u\right]_{31} &= \frac{c' c'' \tilde{y}_6 (z_3 y_b - z_t y_7)}{\sqrt{t_d^q t_s^u} y_5 y_b} \frac{u^2}{\sqrt{t}}, \\
\left[\hat{A}_1^u\right]_{32} &= \frac{c' (z_3 y_b - z_t y_7)}{\sqrt{t_d^q t_s^u} y_b} u, \\
\left[\hat{A}_1^u\right]_{33} &= \frac{z_t}{\sqrt{t_s^q t_s^u}},
\end{aligned} \tag{B.21}$$

while for \hat{A}_2^u we have

$$\begin{aligned}
 [\hat{A}_2^u]_{11} &= \frac{c_{T2}^F y_1}{\sqrt{t_d^q t_d^u}} tu^2, \\
 [\hat{A}_2^u]_{12} &= \left(\frac{c_{T3}^F y_1 + c_{F''}^F y_2}{2\sqrt{t_d^q t_d^u}} - \frac{c^F t_5^u y_1}{2\sqrt{t_d^q t_d^u t_1^u}} + \frac{c^{F'} t_6^u y_3}{\sqrt{t_d^q t_d^u (t_d^u - t_s^u)}} \right) tu^2 - \frac{c^{F'} t_4^u t_5^u y_3}{2\sqrt{t_d^q t_d^u t_1^u (t_d^u - t_s^u)}} u^3, \\
 [\hat{A}_2^u]_{13} &= -\frac{(c^{F'} t_5^u + 2c_{\eta_2}^F t_1^u) y_4}{2\sqrt{t_s^q t_d^u t_1^u}} tu^2, \\
 [\hat{A}_2^u]_{21} &= \frac{c^F c'' y_1 \tilde{y}_6}{\sqrt{t_d^q t_d^u} y_5} \sqrt{t} u^2 + \frac{c^{F'} c'' t_4^u y_3 \tilde{y}_6}{\sqrt{t_d^q t_d^u (t_d^u - t_s^u)} y_5} \frac{u^3}{\sqrt{t}} \\
 [\hat{A}_2^u]_{22} &= \frac{c^F y_1}{\sqrt{t_d^q t_d^u}} tu + \frac{c^{F'} t_4^u y_3}{\sqrt{t_d^q t_d^u (t_d^u - t_s^u)}} u^2, \\
 [\hat{A}_2^u]_{23} &= \frac{c^{F'} y_4}{\sqrt{t_s^q t_d^u}} tu, \\
 [\hat{A}_2^u]_{31} &= \frac{c^{F'} c'' y_3 \tilde{y}_6}{\sqrt{t_d^q t_s^u} y_5} \frac{u^2}{\sqrt{t}}, \\
 [\hat{A}_2^u]_{32} &= \frac{c^{F'} y_3}{\sqrt{t_d^q t_s^u}} u, \\
 [\hat{A}_2^u]_{33} &= \frac{c^{F'} y_3 (c' t_s^q y_7 - t_4^q y_b)}{\sqrt{t_s^q t_s^u t_d^q} y_b} u^2.
 \end{aligned} \tag{B.22}$$

Finally we deal with the down squarks and the contributions are the following:

$$(\hat{m}_{dRL}^2)_1 = \hat{A}_1^d \frac{v \cos \beta}{\sqrt{2}} A_0, \quad (\hat{m}_{dRL}^2)_2 = \hat{A}_2^d \frac{v \cos \beta}{\sqrt{2}} A_0, \tag{B.23}$$

where \hat{A}_1^d is given by

$$\hat{A}_1^d = \begin{pmatrix} -\frac{c''^2 z_5 \tilde{y}_6^2}{\sqrt{t_d^q t_d^d} y_5^2} u^3 & -\frac{c'' z_5 \tilde{y}_6}{\sqrt{t_d^q t_d^d} y_5} \sqrt{t} u^2 & \frac{c' c'' \tilde{y}_6 (z_8 y_b - z_b y_8)}{\sqrt{t_s^q t_d^d} y_5 y_b} \sqrt{t} u^2 \\ \frac{c'' z_5 \tilde{y}_6}{\sqrt{t_d^q t_d^d} y_5} \sqrt{t} u^2 & \frac{z_5}{\sqrt{t_d^q t_d^d}} tu & \frac{c' (z_8 y_b - z_b y_8)}{\sqrt{t_s^q t_d^d} y_b} tu \\ \frac{c' c'' \tilde{y}_6 (z_7 y_b - z_b y_7)}{\sqrt{t_d^q t_s^d} y_5 y_b} \sqrt{t} u^2 & \frac{c' (z_8 y_b - z_b y_8)}{\sqrt{t_d^q t_s^d} y_b} tu & \frac{z_b}{\sqrt{t_s^q t_s^d}} t \end{pmatrix} \tag{B.24}$$

while for \hat{A}_2^d we have

$$\hat{A}_2^d = \begin{pmatrix} \frac{c''(2c^{F''} - c^F c'') \tilde{y}_6^2}{\sqrt{t_d^q t_d^d} y_5} u^3 & \frac{(c^{F''} - c^F c'') \tilde{y}_6}{\sqrt{t_d^q t_d^d}} \sqrt{tu^2} & -\frac{c^{F'} c'' \tilde{y}_6 y_8}{\sqrt{t_s^q t_d^d} y_5} \sqrt{tu^2} \\ -\frac{(c^{F''} - c^F c'') \tilde{y}_6}{\sqrt{t_d^q t_d^d}} \sqrt{tu^2} & \frac{c^F y_5}{\sqrt{t_d^q t_d^d}} tu & \frac{c^{F'} y_8}{\sqrt{t_s^q t_d^d}} tu \\ \frac{c^{F'} c'' \tilde{y}_6 y_7}{\sqrt{t_d^q t_s^d} y_5} \sqrt{tu^2} & \frac{c^{F'} y_7}{\sqrt{t_d^q t_s^d}} tu & [\hat{A}_2^d]_{33} \end{pmatrix} \quad (\text{B.25})$$

where

$$[\hat{A}_2^d]_{33} = \left(\frac{y_8 (c' t_s^d y_8 - t_4^d y_b)}{\sqrt{t_s^q t_s^d t_d^d}} + \frac{y_7 (c' t_s^d y_7 - t_4^q y_b)}{\sqrt{t_s^q t_s^d t_d^d}} \right) \frac{c^{F'} tu^2}{y_b}. \quad (\text{B.26})$$

C Canonical normalisation of the kinetic terms and diagonalisation of $M_{\ell,d}$

We first perform the transformations to go to the basis in which the kinetic terms are canonically normalised and after we diagonalise the charged lepton and the down quark mass matrices. We perform these transformations not only on the fermions, but also on the sfermions in order to ensure that the gaugino-fermion-sfermion vertices do not violate flavour at this stage.

To diagonalise the hermitian matrices K^f , $f = \ell, e, q, u, d$, we apply the unitary transformations W^f :

$$W^{f\dagger} K^f W^f = \text{diag}. \quad (\text{C.1})$$

Normalizing K^f requires a rescaling of the fields via the real (diagonal) matrices R^f :

$$R^f W^{f\dagger} K^f W^f R^f = \mathbb{1}. \quad (\text{C.2})$$

The superfields $\Psi_f = \{\ell, \ell^c, q, q^c\}$ are expressed as

$$\Psi_f = W^f R^f \Psi'_f, \quad (\text{C.3})$$

so that the kinetic terms are in their the canonical form

$$i \bar{\Psi}'_{f,i} \bar{\sigma}^\mu \mathcal{D}_\mu \Psi'_{f,i} + |\mathcal{D}_\mu \tilde{\Psi}'_{f,i}|^2. \quad (\text{C.4})$$

The mass matrices for fermions in this basis read as

$$\begin{aligned} \ell^c M_\ell \ell &= \ell^{c'} R^e (W^e)^T M_\ell W^\ell R^\ell \ell' \equiv \ell^{c'} M'_\ell \ell', \\ U^c M_u Q &= U^{c'} R^u (W^u)^T M_u W^q R^q Q' \equiv U^{c'} M'_u Q', \\ D^c M_d Q &= D^{c'} R^d (W^d)^T M_d W^q R^q Q' \equiv D^{c'} M'_d Q', \end{aligned} \quad (\text{C.5})$$

while for sleptons as

$$\begin{aligned} \tilde{\ell} m_{eLL}^2 \tilde{\ell} &= \tilde{\ell}^c R^\ell (W^\ell)^\dagger m_{eLL}^2 W^\ell R^\ell \tilde{\ell}', \\ \tilde{\ell}^c m_{eRR}^2 \tilde{\ell}^c &= \tilde{\ell}^{c'} R^e (W^e)^T m_{eRR}^2 W^{e*} R^e \tilde{\ell}^{c'}, \\ \tilde{\ell}^c m_{eRL}^2 \tilde{\ell} &= \tilde{\ell}^{c'} R^e (W^e)^T m_{eRL}^2 W^\ell R^\ell \tilde{\ell}', \end{aligned} \quad (\text{C.6})$$

and for quarks as

$$\begin{aligned}
 \bar{Q} m_{qLL}^2 \tilde{Q} &= \bar{Q}' R^q (W^q)^\dagger m_{qLL}^2 W^q R^q \tilde{Q}', \\
 \tilde{U}^c m_{uRR}^2 \bar{U}^c &= \tilde{U}^{c'} R^u (W^u)^T m_{uRR}^2 W^{u*} R^u \bar{U}^{c'}, \\
 \tilde{D}^c m_{dRR}^2 \bar{D}^c &= \tilde{D}^{c'} R^d (W^d)^T m_{dRR}^2 W^{d*} R^d \bar{D}^{c'}, \\
 \tilde{U}^c m_{uRL}^2 \tilde{Q} &= \tilde{U}^{c'} R^u (W^u)^T m_{uRL}^2 W^q R^q \tilde{Q}', \\
 \tilde{D}^c m_{dRL}^2 \tilde{Q} &= \tilde{D}^{c'} R^d (W^d)^T m_{dRL}^2 W^q R^q \tilde{Q}'.
 \end{aligned} \tag{C.7}$$

We diagonalise the resulting mass matrices m'_ℓ and m'_d of the charged leptons and down quarks, respectively, by the usual bi-unitary transformations:

$$\begin{aligned}
 U_e^T M'_\ell V_e &= \text{diag}(m_e, m_\mu, m_\tau), \\
 U_d^T M'_d V_d &= \text{diag}(m_d, m_s, m_b).
 \end{aligned} \tag{C.8}$$

In this way we can define the mass eigenbasis ℓ'' , $\ell^{c''}$, Q'' , $D^{c''}$:

$$\ell' = V_e \ell'', \quad \ell^{c'} = U_e \ell^{c''}, \quad Q' = V_d Q'', \quad D^{c'} = U_d D^{c''}. \tag{C.9}$$

Finally, the slepton mass matrices are given by

$$\begin{aligned}
 \bar{\tilde{\ell}} m_{eLL}^2 \tilde{\ell} &= \bar{\tilde{\ell}}'' \left[V_e^\dagger R^\ell W^{\ell\dagger} m_{eLL}^2 W^\ell R^\ell V_e \right] \tilde{\ell}'' \equiv \bar{\tilde{\ell}}'' \hat{m}_{eLL}^2 \tilde{\ell}'', \\
 \tilde{\ell}^c m_{eRR}^2 \bar{\tilde{\ell}}^c &= \tilde{\ell}^{c''} \left[U_e^T R^e (W^e)^T m_{eRR}^2 W^{e*} R^e U_e \right] \bar{\tilde{\ell}}^{c''} \equiv \tilde{\ell}^{c''} \hat{m}_{eRR}^2 \bar{\tilde{\ell}}^{c''}, \\
 \tilde{\ell}^c m_{eRL}^2 \tilde{\ell} &= \tilde{\ell}^{c''} \left[U_e^T R^e (W^e)^T m_{eRL}^2 W^\ell R^\ell V_e \right] \tilde{\ell}'' \equiv \tilde{\ell}^{c''} \hat{m}_{eRL}^2 \tilde{\ell}'',
 \end{aligned} \tag{C.10}$$

and the squark ones by

$$\begin{aligned}
 \bar{Q} m_{qLL}^2 \tilde{Q} &= \bar{Q}'' \left[V_d^\dagger R^q (W^q)^\dagger m_{qLL}^2 W^q R^q V_d \right] \tilde{Q}'', \\
 \tilde{D}^c m_{dRR}^2 \bar{D}^c &= \tilde{D}^{c''} \left[U_d^T R^d (W^d)^T m_{dRR}^2 W^{d*} R^d U_d \right] \bar{D}^{c''}, \\
 \tilde{U}^c m_{uRL}^2 \tilde{Q} &= \tilde{U}^{c'} \left[R^u (W^u)^T m_{uRL}^2 W^q R^q V_d \right] \tilde{Q}'', \\
 \tilde{D}^c m_{dRL}^2 \tilde{Q} &= \tilde{D}^{c''} \left[U_d^T R^d (W^d)^T m_{dRL}^2 W^q R^q V_d \right] \tilde{Q}''.
 \end{aligned} \tag{C.11}$$

Note that the m_{uRR}^2 has been not affected by these last transformations.

To arrive at this result we assume that all couplings involved are real and as a result the matrices W^f , $U_{e,d}$ and $V_{e,d}$ turn out to be orthogonal instead of unitary.

D Wilson coefficient contributions for $\text{BR}(\bar{B} \rightarrow X_s \gamma)$

In this appendix we report the break down of the $C_{7\gamma}$ Wilson coefficient for $\text{BR}(\bar{B} \rightarrow X_s \gamma)$ in terms of the distinct supersymmetric contributions. In figure 9, the two upper (lower) plots refer to $A_0 = 2 m_0 = 400 \text{ GeV}$ ($A_0 = 2 m_0 = 2000 \text{ GeV}$), respectively for the RP_A case (left) and RP_B case (right). The different colors refer to distinct contributions: Magenta (Red) for the chargino contribution with positive (negative) $\text{sign}[\mu]$; Black (Cyan) for the

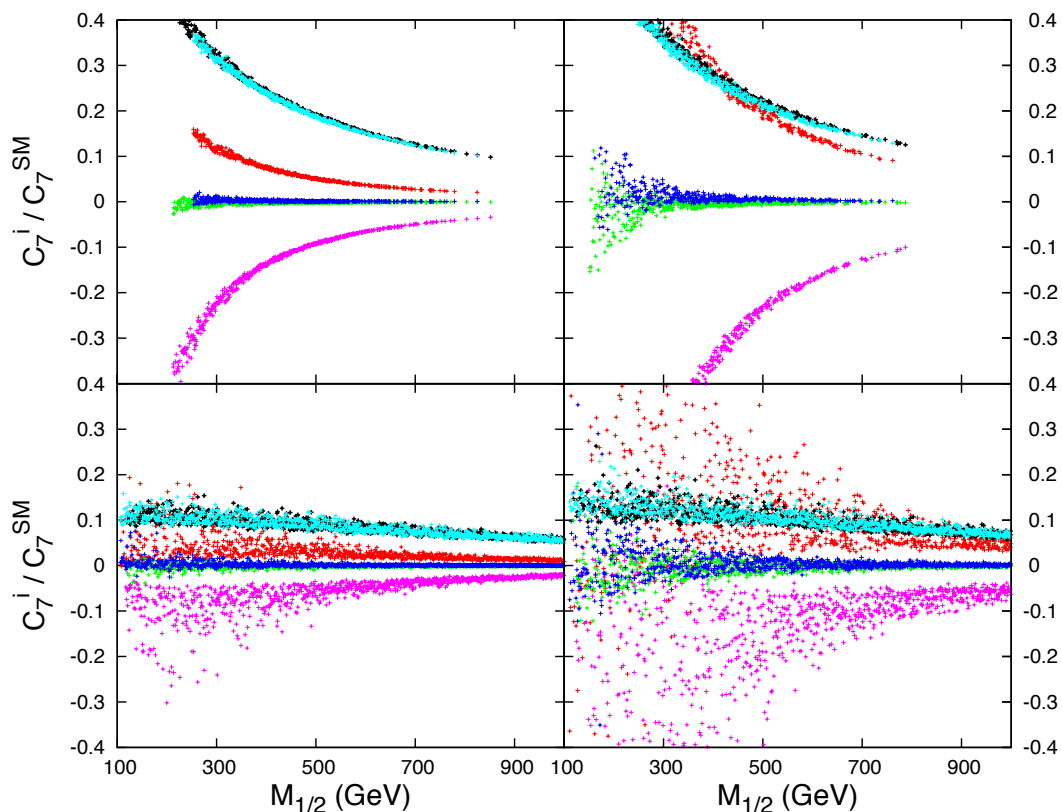


Figure 9. Wilson coefficient contributions for $\text{BR}(\bar{B} \rightarrow X_s \gamma)$. The left (right) plots refer to the RP_A (RP_B) case for $A_0 = 2m_0 = 400$ GeV (upper plots) or $A_0 = 2m_0 = 2000$ GeV (lower plots). See the text for details.

charged Higgs contribution with positive (negative) $\text{sign}[\mu]$; Green (Blue) for the gluino contribution with positive (negative) $\text{sign}[\mu]$.

Figure 9 confirms the analysis reported in section 5.3: in the small (A_0, m_0) region (upper plots) the dominant T' contribution to the $b \rightarrow s \gamma$ BR is typically the charged Higgs one, that is always concordant in sign with the SM one. The second most relevant contribution is the chargino one with a sign depending on $\text{sign}[\mu]$: it tends to enhance (cancel) the SM contribution for $\mu < 0$ ($\mu > 0$). Gluino contributions are practically independent from $\text{sign}[\mu]$. In figure 9 we do not show the neutralino contribution, since it turns out to be completely negligible.

References

- [1] F. Feruglio, C. Hagedorn, Y. Lin and L. Merlo, *Tri-bimaximal neutrino mixing and quark masses from a discrete flavour symmetry*, *Nucl. Phys. B* **775** (2007) 120 [[hep-ph/0702194](#)] [[INSPIRE](#)].
- [2] PARTICLE DATA GROUP collaboration, K. Nakamura et al., *Review of particle physics*, *J. Phys. G* **37** (2010) 075021 [[INSPIRE](#)].

- [3] T2K COLLABORATION collaboration, K. Abe et al., *Indication of electron neutrino appearance from an accelerator-produced off-axis muon neutrino beam*, *Phys. Rev. Lett.* **107** (2011) 041801 [[arXiv:1106.2822](#)] [[INSPIRE](#)].
- [4] G. Fogli, E. Lisi, A. Marrone, A. Palazzo and A. Rotunno, *Evidence of $\theta_{13} \neq 0$ from global neutrino data analysis*, *Phys. Rev. D* **84** (2011) 053007 [[arXiv:1106.6028](#)] [[INSPIRE](#)].
- [5] T. Schwetz, M. Tortola and J. Valle, *Global neutrino data and recent reactor fluxes: status of three-flavour oscillation parameters*, *New J. Phys.* **13** (2011) 063004 [[arXiv:1103.0734](#)] [[INSPIRE](#)].
- [6] P. Harrison, D. Perkins and W. Scott, *Tri-bimaximal mixing and the neutrino oscillation data*, *Phys. Lett. B* **530** (2002) 167 [[hep-ph/0202074](#)] [[INSPIRE](#)].
- [7] P. Harrison and W. Scott, *Symmetries and generalizations of tri-bimaximal neutrino mixing*, *Phys. Lett. B* **535** (2002) 163 [[hep-ph/0203209](#)] [[INSPIRE](#)].
- [8] Z.-z. Xing, *Nearly tri bimaximal neutrino mixing and CP-violation*, *Phys. Lett. B* **533** (2002) 85 [[hep-ph/0204049](#)] [[INSPIRE](#)].
- [9] F. Vissani, *A study of the scenario with nearly degenerate Majorana neutrinos*, [hep-ph/9708483](#) [[INSPIRE](#)].
- [10] V.D. Barger, S. Pakvasa, T.J. Weiler and K. Whisnant, *Bimaximal mixing of three neutrinos*, *Phys. Lett. B* **437** (1998) 107 [[hep-ph/9806387](#)] [[INSPIRE](#)].
- [11] G. Altarelli and F. Feruglio, *Neutrino mass textures from oscillations with maximal mixing*, *Phys. Lett. B* **439** (1998) 112 [[hep-ph/9807353](#)] [[INSPIRE](#)].
- [12] R.N. Mohapatra and S. Nussinov, *Bimaximal neutrino mixing and neutrino mass matrix*, *Phys. Rev. D* **60** (1999) 013002 [[hep-ph/9809415](#)] [[INSPIRE](#)].
- [13] I. Stancu and D.V.a. Ahluwalia, *L/E flatness of the electron-like event ratio in super-kamiokande and a degeneracy in neutrino masses*, *Phys. Lett. B* **460** (1999) 431 [[hep-ph/9903408](#)] [[INSPIRE](#)].
- [14] Y. Kajiyama, M. Raidal and A. Strumia, *The golden ratio prediction for the solar neutrino mixing*, *Phys. Rev. D* **76** (2007) 117301 [[arXiv:0705.4559](#)] [[INSPIRE](#)].
- [15] W. Rodejohann, *Unified parametrization for quark and lepton mixing angles*, *Phys. Lett. B* **671** (2009) 267 [[arXiv:0810.5239](#)] [[INSPIRE](#)].
- [16] G. D'Ambrosio, G. Giudice, G. Isidori and A. Strumia, *Minimal flavor violation: an effective field theory approach*, *Nucl. Phys. B* **645** (2002) 155 [[hep-ph/0207036](#)] [[INSPIRE](#)].
- [17] V. Cirigliano, B. Grinstein, G. Isidori and M.B. Wise, *Minimal flavor violation in the lepton sector*, *Nucl. Phys. B* **728** (2005) 121 [[hep-ph/0507001](#)] [[INSPIRE](#)].
- [18] S. Davidson and F. Palorini, *Various definitions of minimal flavour violation for leptons*, *Phys. Lett. B* **642** (2006) 72 [[hep-ph/0607329](#)] [[INSPIRE](#)].
- [19] R. Alonso, G. Isidori, L. Merlo, L.A. Muñoz and E. Nardi, *Minimal flavour violation extensions of the seesaw*, *JHEP* **06** (2011) 037 [[arXiv:1103.5461](#)] [[INSPIRE](#)].
- [20] B. Grinstein, M. Redi and G. Villadoro, *Low scale flavor gauge symmetries*, *JHEP* **11** (2010) 067 [[arXiv:1009.2049](#)] [[INSPIRE](#)].
- [21] T. Feldmann, *See-saw masses for quarks and leptons in SU(5)*, *JHEP* **04** (2011) 043 [[arXiv:1010.2116](#)] [[INSPIRE](#)].

- [22] D. Guadagnoli, R.N. Mohapatra and I. Sung, *Gauged flavor group with left-right symmetry*, *JHEP* **04** (2011) 093 [[arXiv:1103.4170](#)] [[INSPIRE](#)].
- [23] A.J. Buras, L. Merlo and E. Stamou, *The impact of flavour changing neutral gauge bosons on $\bar{b} \rightarrow X_s \gamma$* , *JHEP* **08** (2011) 124 [[arXiv:1105.5146](#)] [[INSPIRE](#)].
- [24] T. Feldmann, M. Jung and T. Mannel, *Sequential flavour symmetry breaking*, *Phys. Rev. D* **80** (2009) 033003 [[arXiv:0906.1523](#)] [[INSPIRE](#)].
- [25] R. Alonso, M. Gavela, L. Merlo and S. Rigolin, *On the scalar potential of minimal flavour violation*, *JHEP* **07** (2011) 012 [[arXiv:1103.2915](#)] [[INSPIRE](#)].
- [26] A. Pomarol and D. Tommasini, *Horizontal symmetries for the supersymmetric flavor problem*, *Nucl. Phys. B* **466** (1996) 3 [[hep-ph/9507462](#)] [[INSPIRE](#)].
- [27] R. Barbieri, G. Dvali and L.J. Hall, *Predictions from a $U(2)$ flavor symmetry in supersymmetric theories*, *Phys. Lett. B* **377** (1996) 76 [[hep-ph/9512388](#)] [[INSPIRE](#)].
- [28] R. Barbieri, L.J. Hall, S. Raby and A. Romanino, *Unified theories with $U(2)$ flavor symmetry*, *Nucl. Phys. B* **493** (1997) 3 [[hep-ph/9610449](#)] [[INSPIRE](#)].
- [29] R. Barbieri, G. Isidori, J. Jones-Perez, P. Lodone and D.M. Straub, *$U(2)$ and minimal flavour violation in supersymmetry*, *Eur. Phys. J. C* **71** (2011) 1725 [[arXiv:1105.2296](#)] [[INSPIRE](#)].
- [30] A. Crivellin, L. Hofer, U. Nierste and D. Scherer, *Phenomenological consequences of radiative flavor violation in the MSSM*, *Phys. Rev. D* **84** (2011) 035030 [[arXiv:1105.2818](#)] [[INSPIRE](#)].
- [31] S. King and G.G. Ross, *Fermion masses and mixing angles from $SU(3)$ family symmetry*, *Phys. Lett. B* **520** (2001) 243 [[hep-ph/0108112](#)] [[INSPIRE](#)].
- [32] J. Chkareuli, C. Froggatt and H. Nielsen, *Minimal mixing of quarks and leptons in the $SU(3)$ theory of flavor*, *Nucl. Phys. B* **626** (2002) 307 [[hep-ph/0109156](#)] [[INSPIRE](#)].
- [33] G.G. Ross and L. Velasco-Sevilla, *Symmetries and fermion masses*, *Nucl. Phys. B* **653** (2003) 3 [[hep-ph/0208218](#)] [[INSPIRE](#)].
- [34] S. King and G.G. Ross, *Fermion masses and mixing angles from $SU(3)$ family symmetry and unification*, *Phys. Lett. B* **574** (2003) 239 [[hep-ph/0307190](#)] [[INSPIRE](#)].
- [35] I. de Medeiros Varzielas and G.G. Ross, *$SU(3)$ family symmetry and neutrino bi-tri-maximal mixing*, *Nucl. Phys. B* **733** (2006) 31 [[hep-ph/0507176](#)] [[INSPIRE](#)].
- [36] E. Ma and G. Rajasekaran, *Softly broken A_4 symmetry for nearly degenerate neutrino masses*, *Phys. Rev. D* **64** (2001) 113012 [[hep-ph/0106291](#)] [[INSPIRE](#)].
- [37] K. Babu, E. Ma and J. Valle, *Underlying A_4 symmetry for the neutrino mass matrix and the quark mixing matrix*, *Phys. Lett. B* **552** (2003) 207 [[hep-ph/0206292](#)] [[INSPIRE](#)].
- [38] G. Altarelli and F. Feruglio, *Tri-bimaximal neutrino mixing from discrete symmetry in extra dimensions*, *Nucl. Phys. B* **720** (2005) 64 [[hep-ph/0504165](#)] [[INSPIRE](#)].
- [39] G. Altarelli and F. Feruglio, *Tri-bimaximal neutrino mixing, A_4 and the modular symmetry*, *Nucl. Phys. B* **741** (2006) 215 [[hep-ph/0512103](#)] [[INSPIRE](#)].
- [40] G. Altarelli, F. Feruglio and Y. Lin, *Tri-bimaximal neutrino mixing from orbifolding*, *Nucl. Phys. B* **775** (2007) 31 [[hep-ph/0610165](#)] [[INSPIRE](#)].
- [41] G. Altarelli and F. Feruglio, *Discrete flavor symmetries and models of neutrino mixing*, *Rev. Mod. Phys.* **82** (2010) 2701 [[arXiv:1002.0211](#)] [[INSPIRE](#)].

- [42] G. Altarelli, F. Feruglio and L. Merlo, *Revisiting bimaximal neutrino mixing in a model with S^4 discrete symmetry*, *JHEP* **05** (2009) 020 [[arXiv:0903.1940](#)] [[INSPIRE](#)].
- [43] R. de Adelhart Toorop, F. Bazzocchi and L. Merlo, *The interplay between GUT and flavour symmetries in a $Pati-Salam \times S^4$ model*, *JHEP* **08** (2010) 001 [[arXiv:1003.4502](#)] [[INSPIRE](#)].
- [44] L.L. Everett and A.J. Stuart, *Icosahedral (A_5) family symmetry and the golden ratio prediction for solar neutrino mixing*, *Phys. Rev. D* **79** (2009) 085005 [[arXiv:0812.1057](#)] [[INSPIRE](#)].
- [45] F. Feruglio and A. Paris, *The golden ratio prediction for the solar angle from a natural model with a_5 flavour symmetry*, *JHEP* **03** (2011) 101 [[arXiv:1101.0393](#)] [[INSPIRE](#)].
- [46] K. Hamaguchi, M. Kakizaki and M. Yamaguchi, *Democratic (s)fermions and lepton flavor violation*, *Phys. Rev. D* **68** (2003) 056007 [[hep-ph/0212172](#)] [[INSPIRE](#)].
- [47] A. Mondragon, M. Mondragon and E. Peinado, *Lepton masses, mixings and FCNC in a minimal S_3 -invariant extension of the standard model*, *Phys. Rev. D* **76** (2007) 076003 [[arXiv:0706.0354](#)] [[INSPIRE](#)].
- [48] N. Kifune, J. Kubo and A. Lenz, *Flavor changing neutral Higgs bosons in a supersymmetric extension based on a Q_6 family symmetry*, *Phys. Rev. D* **77** (2008) 076010 [[arXiv:0712.0503](#)] [[INSPIRE](#)].
- [49] H. Ishimori, T. Kobayashi, H. Ohki, Y. Omura, R. Takahashi, et al., *Soft supersymmetry breaking terms from $D_4 \times Z_2$ lepton flavor symmetry*, *Phys. Rev. D* **77** (2008) 115005 [[arXiv:0803.0796](#)] [[INSPIRE](#)].
- [50] H. Ishimori, T. Kobayashi, Y. Omura and M. Tanimoto, *Soft supersymmetry breaking terms from A_4 lepton flavor symmetry*, *JHEP* **12** (2008) 082 [[arXiv:0807.4625](#)] [[INSPIRE](#)].
- [51] H. Ishimori, T. Kobayashi, H. Okada, Y. Shimizu and M. Tanimoto, *Δ_{54} flavor model for leptons and sleptons*, *JHEP* **12** (2009) 054 [[arXiv:0907.2006](#)] [[INSPIRE](#)].
- [52] C.M. Ho and T.W. Kephart, *Electron and muon $g - 2$ contributions from the T' Higgs sector*, *Phys. Lett. B* **687** (2010) 201 [[arXiv:1001.3696](#)] [[INSPIRE](#)].
- [53] P.H. Frampton, C.M. Ho, T.W. Kephart and S. Matsuzaki, *LHC Higgs production and decay in the T' model*, *Phys. Rev. D* **82** (2010) 113007 [[arXiv:1009.0307](#)] [[INSPIRE](#)].
- [54] R. de Adelhart Toorop, F. Bazzocchi, L. Merlo and A. Paris, *Constraining flavour symmetries at the ew scale I: the A_4 Higgs potential*, *JHEP* **03** (2011) 035 [[arXiv:1012.1791](#)] [[INSPIRE](#)].
- [55] R. de Adelhart Toorop, F. Bazzocchi, L. Merlo and A. Paris, *Constraining flavour symmetries at the ew scale II: the fermion processes*, *JHEP* **03** (2011) 040 [[arXiv:1012.2091](#)] [[INSPIRE](#)].
- [56] F. Feruglio, C. Hagedorn, Y. Lin and L. Merlo, *Lepton flavour violation in models with A_4 flavour symmetry*, *Nucl. Phys. B* **809** (2009) 218 [[arXiv:0807.3160](#)] [[INSPIRE](#)].
- [57] F. Feruglio, C. Hagedorn, Y. Lin and L. Merlo, *Theory of the neutrino mass*, in the proceedings of *IV International Workshop on Neutrino Oscillations*, Venice Italy, M. Baldo Ceolin ed., Papergraf Edition, Padova Italy (2008) 29 [[arXiv:0808.0812](#)] [[INSPIRE](#)].
- [58] F. Feruglio, C. Hagedorn and L. Merlo, *Vacuum alignment in SUSY A_4 models*, *JHEP* **03** (2010) 084 [[arXiv:0910.4058](#)] [[INSPIRE](#)].

- [59] Y. Lin, L. Merlo and A. Paris, *Running effects on lepton mixing angles in flavour models with type I seesaw*, *Nucl. Phys. B* **835** (2010) 238 [[arXiv:0911.3037](#)] [[INSPIRE](#)].
- [60] F. Feruglio, C. Hagedorn, Y. Lin and L. Merlo, *Lepton flavour violation in a supersymmetric model with A_4 flavour symmetry*, *Nucl. Phys. B* **832** (2010) 251 [[arXiv:0911.3874](#)] [[INSPIRE](#)].
- [61] F. Feruglio and A. Paris, *Rare muon and τ decays in A_4 models*, *Nucl. Phys. B* **840** (2010) 405 [[arXiv:1005.5526](#)] [[INSPIRE](#)].
- [62] G. Isidori, Y. Nir and G. Perez, *Flavor physics constraints for physics beyond the standard model*, *Ann. Rev. Nucl. Part. Sci.* **60** (2010) 355 [[arXiv:1002.0900](#)] [[INSPIRE](#)].
- [63] C. Froggatt and H.B. Nielsen, *Hierarchy of quark masses, Cabibbo angles and CP-violation*, *Nucl. Phys. B* **147** (1979) 277 [[INSPIRE](#)].
- [64] G.G. Ross and O. Vives, *Yukawa structure, flavor and CP-violation in supergravity*, *Phys. Rev. D* **67** (2003) 095013 [[hep-ph/0211279](#)] [[INSPIRE](#)].
- [65] M.A. Luty, *2004 TASI lectures on supersymmetry breaking*, [hep-th/0509029](#) [[INSPIRE](#)].
- [66] W. Porod, *SPheno, a program for calculating supersymmetric spectra, SUSY particle decays and SUSY particle production at e^+e^- colliders*, *Comput. Phys. Commun.* **153** (2003) 275 [[hep-ph/0301101](#)] [[INSPIRE](#)].
- [67] MEG COLLABORATION collaboration, J. Adam et al., *New limit on the lepton-flavour violating decay $\mu^+ \rightarrow e^+\gamma$* , [arXiv:1107.5547](#) [[INSPIRE](#)].
- [68] P. Paradisi, *Constraints on SUSY lepton flavor violation by rare processes*, *JHEP* **10** (2005) 006 [[hep-ph/0505046](#)] [[INSPIRE](#)].
- [69] W. Hollik, J.I. Illana, S. Rigolin and D. Stöckinger, *One loop MSSM contribution to the weak magnetic dipole moments of heavy fermions*, *Phys. Lett. B* **416** (1998) 345 [[hep-ph/9707437](#)] [[INSPIRE](#)].
- [70] W. Hollik, J.I. Illana, S. Rigolin and D. Stöckinger, *Weak electric dipole moments of heavy fermions in the MSSM*, *Phys. Lett. B* **425** (1998) 322 [[hep-ph/9711322](#)] [[INSPIRE](#)].
- [71] L.L. Everett, G.L. Kane, S. Rigolin, L.-T. Wang and T.T. Wang, *Alternative approach to $b \rightarrow s\gamma$ in the uMSSM*, *JHEP* **01** (2002) 022 [[hep-ph/0112126](#)] [[INSPIRE](#)].
- [72] M. Misiak, H. Asatrian, K. Bieri, M. Czakon, A. Czarnecki, et al., *Estimate of $B(\bar{B} \rightarrow X_s \gamma)$ at $o(\alpha_s^2)$* , *Phys. Rev. Lett.* **98** (2007) 022002 [[hep-ph/0609232](#)] [[INSPIRE](#)].
- [73] P. Gambino and M. Misiak, *Quark mass effects in $\bar{B} \rightarrow X_s \gamma$* , *Nucl. Phys. B* **611** (2001) 338 [[hep-ph/0104034](#)] [[INSPIRE](#)].
- [74] M. Misiak and M. Steinhauser, *NNLO QCD corrections to the $\bar{B} \rightarrow X_s \gamma$ matrix elements using interpolation in m_c* , *Nucl. Phys. B* **764** (2007) 62 [[hep-ph/0609241](#)] [[INSPIRE](#)].
- [75] A. Lenz, U. Nierste, J. Charles, S. Descotes-Genon, A. Jantsch, et al., *Anatomy of new physics in $B - \bar{B}$ mixing*, *Phys. Rev. D* **83** (2011) 036004 [[arXiv:1008.1593](#)] [[INSPIRE](#)].